REPORT DOCUMENTATION PAGE

Form Approved
OMB No. 0704-0188

PLEASE DO NOT RETURN YOUR FORM TO THE ABOVE ORGANIZATION.

1. REPORT DATE *(DD-MM-YYYY)*	2. REPORT TYPE	3. DATES COVERED *(From - To)*
15/08/2005	Final Technical Report	August 15, 2005-August 14, 2006

4. TITLE AND SUBTITLE

Prediction of Texture and Formability of
Continuous Cast AA 5000 and 2000 Series Aluminum Alloy
Sheets and Their Quality Improvement

5a. CONTRACT NUMBER

5b. GRANT NUMBER

FA 9550-04-1-0457

5c. PROGRAM ELEMENT NUMBER

6. AUTHOR(S)

Prof. James G. Morris

5d. PROJECT NUMBER

5e. TASK NUMBER

5f. WORK UNIT NUMBER

7. PERFORMING ORGANIZATION NAME(S) AND ADDRESS(ES)

University of Kentucky, Department of Chemical and Materials Engineering
177 Anderson Hall
Lexington, KY 40506-0046

8. PERFORMING ORGANIZATION REPORT NUMBER

N/A

9. SPONSORING/MONITORING AGENCY NAME(S) AND ADDRESS(ES)

Air Force Office of Scientific Research
875 N. Randolph Street
Arlington, VA 22203

10. SPONSOR/MONITOR'S ACRONYM(S)

AFOSR

11. SPONSOR/MONITOR'S REPORT NUMBER(S)

AFRL-AFOSR-VA-TR-2016-0601

12. DISTRIBUTION/AVAILABILITY STATEMENT

Unclassified Unlimited

13. SUPPLEMENTARY NOTES

14. ABSTRACT

The goal of this research is concerned with the following:
To study the effect of processing parameters on micro-structure, texture and formability of selected AA 5000 and AA 3000 series aluminum alloys and of AA 2037 aluminum alloy. To determine quantitatively the texture evolution of the above mentioned alloys during cold rolling. The equations of the texture volume fractions and true rolling strain will be established in order to predict the texture evolution during rolling. Our work will focus on the effect of initial micro-structure and texture on the subsequent texture evolution.

15. SUBJECT TERMS

16. SECURITY CLASSIFICATION OF:			17. LIMITATION OF ABSTRACT	18. NUMBER OF PAGES	19a. NAME OF RESPONSIBLE PERSON
a. REPORT	b. ABSTRACT	c. THIS PAGE			James G. Morris
unclassified	unclassified	unclassified			19b. TELEPHONE NUMBER *(Include area code)* (859) 257-8090

INSTRUCTIONS FOR COMPLETING SF 298

1. REPORT DATE. Full publication date, including day, month, if available. Must cite at least the year and be Year 2000 compliant, e.g. 30-06-1998; xx-06-1998; xx-xx-1998.

2. REPORT TYPE. State the type of report, such as final, technical, interim, memorandum, master's thesis, progress, quarterly, research, special, group study, etc.

3. DATES COVERED. Indicate the time during which the work was performed and the report was written, e.g., Jun 1997 - Jun 1998; 1-10 Jun 1996; May - Nov 1998; Nov 1998.

4. TITLE. Enter title and subtitle with volume number and part number, if applicable. On classified documents, enter the title classification in parentheses.

5a. CONTRACT NUMBER. Enter all contract numbers as they appear in the report, e.g. F33615-86-C-5169.

5b. GRANT NUMBER. Enter all grant numbers as they appear in the report, e.g. AFOSR-82-1234.

5c. PROGRAM ELEMENT NUMBER. Enter all program element numbers as they appear in the report, e.g. 61101A.

5d. PROJECT NUMBER. Enter all project numbers as they appear in the report, e.g. 1F665702D1257; ILIR.

5e. TASK NUMBER. Enter all task numbers as they appear in the report, e.g. 05; RF0330201; T4112.

5f. WORK UNIT NUMBER. Enter all work unit numbers as they appear in the report, e.g. 001; AFAPL30480105.

6. AUTHOR(S). Enter name(s) of person(s) responsible for writing the report, performing the research, or credited with the content of the report. The form of entry is the last name, first name, middle initial, and additional qualifiers separated by commas, e.g. Smith, Richard, J, Jr.

7. PERFORMING ORGANIZATION NAME(S) AND ADDRESS(ES). Self-explanatory.

8. PERFORMING ORGANIZATION REPORT NUMBER. Enter all unique alphanumeric report numbers assigned by the performing organization, e.g. BRL-1234; AFWL-TR-85-4017-Vol-21-PT-2.

9. SPONSORING/MONITORING AGENCY NAME(S) AND ADDRESS(ES). Enter the name and address of the organization(s) financially responsible for and monitoring the work.

10. SPONSOR/MONITOR'S ACRONYM(S). Enter, if available, e.g. BRL, ARDEC, NADC.

11. SPONSOR/MONITOR'S REPORT NUMBER(S). Enter report number as assigned by the sponsoring/ monitoring agency, if available, e.g. BRL-TR-829; -215.

12. DISTRIBUTION/AVAILABILITY STATEMENT. Use agency-mandated availability statements to indicate the public availability or distribution limitations of the report. If additional limitations/ restrictions or special markings are indicated, follow agency authorization procedures, e.g. RD/FRD, PROPIN, ITAR, etc. Include copyright information.

13. SUPPLEMENTARY NOTES. Enter information not included elsewhere such as: prepared in cooperation with; translation of; report supersedes; old edition number, etc.

14. ABSTRACT. A brief (approximately 200 words) factual summary of the most significant information.

15. SUBJECT TERMS. Key words or phrases identifying major concepts in the report.

16. SECURITY CLASSIFICATION. Enter security classification in accordance with security classification regulations, e.g. U, C, S, etc. If this form contains classified information, stamp classification level on the top and bottom of this page.

17. LIMITATION OF ABSTRACT. This block must be completed to assign a distribution limitation to the abstract. Enter UU (Unclassified Unlimited) or SAR (Same as Report). An entry in this block is necessary if the abstract is to be limited.

Part III. Effect of Pre-heat Treatment on the Evolution of Recrystallization and Recrystallization Textures in CC AA 3105 Aluminum Alloy

Wenchang Liu, James G. Morris, and Chi-Sing Man

1. Introduction

Recrystallization texture has long been a subject of research by metallurgists since it is one of the main factors responsible for the anisotropy of mechanical properties of final sheet products. The recrystallization textures of most aluminum alloys are dominated by the cube orientation with strong scatter about the rolling direction (RD) towards the Goss orientation. However, annealing of deformed supersaturated AA 3xxx series aluminum alloys usually results in different recrystallization textures due to the effect of concurrent precipitation [1,4]. The effect of concurrent precipitation on recrystallization and recrystallization texture has been reported [2,3,5,27,28]. It was found that concurrent precipitation significantly retarded the recrystallization of AA 3003 aluminum alloy [27,28]. Large flat grains aligned with the rolling direction in a supersaturated Al-1.3%Mn alloy were attributed to preferred nucleation of precipitation on large and low angle grain boundaries [5]. Several papers have focused on the evolution of recrystallization texture during concurrent precipitation [1,2,4]. It was found that concurrent precipitation resulted in relatively strong P {011}<455> and ND-rotated cube {001}<310> textures in commercial Al-Mn-Mg [1] and Al-Mn [4] alloys. According to Engler and co-workers [15,16], this enhanced P and ND-rotated cube textures originated from particle stimulated nucleation of recrystallization. These orientations were a result of microgrowth selection, taking place in the deformation zone around the largest particles.

CC hot bands retain a large amount of alloying elements in solid solution due to the rapid cooling rate of the CC slab. The microstructure and texture of CC hot bands as well as the supersaturation of solute elements in the matrix can be altered by heat treatments prior to cold rolling. Different precipitation states and different degrees of solute supersaturation strongly affect the evolution of microstructure and recrystallization texture during subsequent annealing. The aim of the present study was to investigate the effect of large particles and small dispersoids - either already present in the as-deformed state or precipitating during the recrystallization anneal - on the evolution of recrystallization and recrystallization textures in CC AA 3105 aluminum alloy.

2. Experimental

The material used in the present investigation was CC AA 3105 aluminum alloy. The CC hot band possessed a typical deformed structure and retained a large amount of alloying elements in solid solution due to the rapid cooling rate of the CC slab. In order to investigate the effect of heat treatment prior to cold rolling on recrystallization and recrystallization texture, the hot band of CC AA 3105 aluminum alloy was preheat treated at (a) 599°C for 6 h (B condition), (b) 482°C for 6 h (D condition), (c) 371°C for 6 h (F condition), and (d) 599°C for 6 h + 371°C for 6 h (G condition), and then followed by water quenching. The hot band (A condition) and preheated hot

bands were subsequently cold rolled to 75% reduction in thickness, and then annealed at different temperatures for various lengths of time in a salt bath, followed by water quenching.

The microstructure of the cold rolled and annealed samples was revealed by anodization and observed under polarized light in an optical microscope. All micrographs were taken from longitudinal sections as defined by the RD and the ND. The hardness was measured using a Buehler Micromet II digital micro hardness tester with a load of 500g in order to reveal the annealing behavior of cold rolled aluminum alloys. Texture measurements were performed at the quarter thickness of the cold rolled and annealed sheets. The volume fractions of the texture components were calculated by an improved integration method [8-10].

3. Results

3.1. Recrystallization of cold rolled samples

3.1.1. Development of Hardness

The progress of recrystallization was studied by measurements of hardness *HV* as a function of annealing time at different temperatures. Fig. 12 shows the variation in hardness with annealing time at different temperatures for cold rolled AA 3105 aluminum alloy with different pre-treatments. It is noted that cold rolled CC AA 3105 aluminum alloy with different pre-treatments exhibited completely different annealing behaviors. Under the A condition, i.e. in the case of no pre-treatment, the hardness decreased gradually during annealing at temperatures below 427°C (Fig. 12(a)). It can not be determined only from the curves of hardness and time when recrystallization started and ended. At 454 and 482°C the alloy was fully recrystallized after 1 min and 2 s, respectively.

Under the B condition, the curves of hardness and time followed a similar variation to materials exhibiting discontinuous recrystallization (Fig. 12(b)). After a minor hardness decrease due to recovery effects, the hardness substantially decreased, indicating the occurrence of primary recrystallization. After complete recrystallization, the hardness decreased slightly with increasing annealing time. The time to reach 50% recrystallization decreased with increasing annealing temperature.

Under the D condition, the hardness decreased gradually at 316°C with increasing annealing time. Recrystallization did not occur when the annealing time was less than 2 days (Fig. 12(c)). At 343°C, the hardness decreased gradually with increasing annealing time. It was determined from measurements of textures that recrystallization started after annealing for about 5 min. Recrystallization proceeded slowly at this temperature in contrast to Fig. 12(b). At 399°C and 427°C the hardness decreased to a low level value after about 1 min and 10 s, respectively.

Under the F condition, the curves of hardness and time seemed to be similar to those under the D condition although their initial microstructure and texture prior to cold rolling were completely different. At a given annealing temperature, recrystallization proceeded slightly more quickly in Fig. 12(d) than in Fig. 12(c).

Under the G condition, the shape of the curves of hardness and time was similar to that in Fig. 12(b). However, the additional heat treatment at 371°C affected their annealing behavior. The time to 50% recrystallization for the cold rolled sheet with the dual pre-treatment was shorter that for the cold rolled sheet with the single pre-treatment. This indicates that particular precipitates produced by the additional heat treatment stimulate recrystallization of the cold rolled sheets.

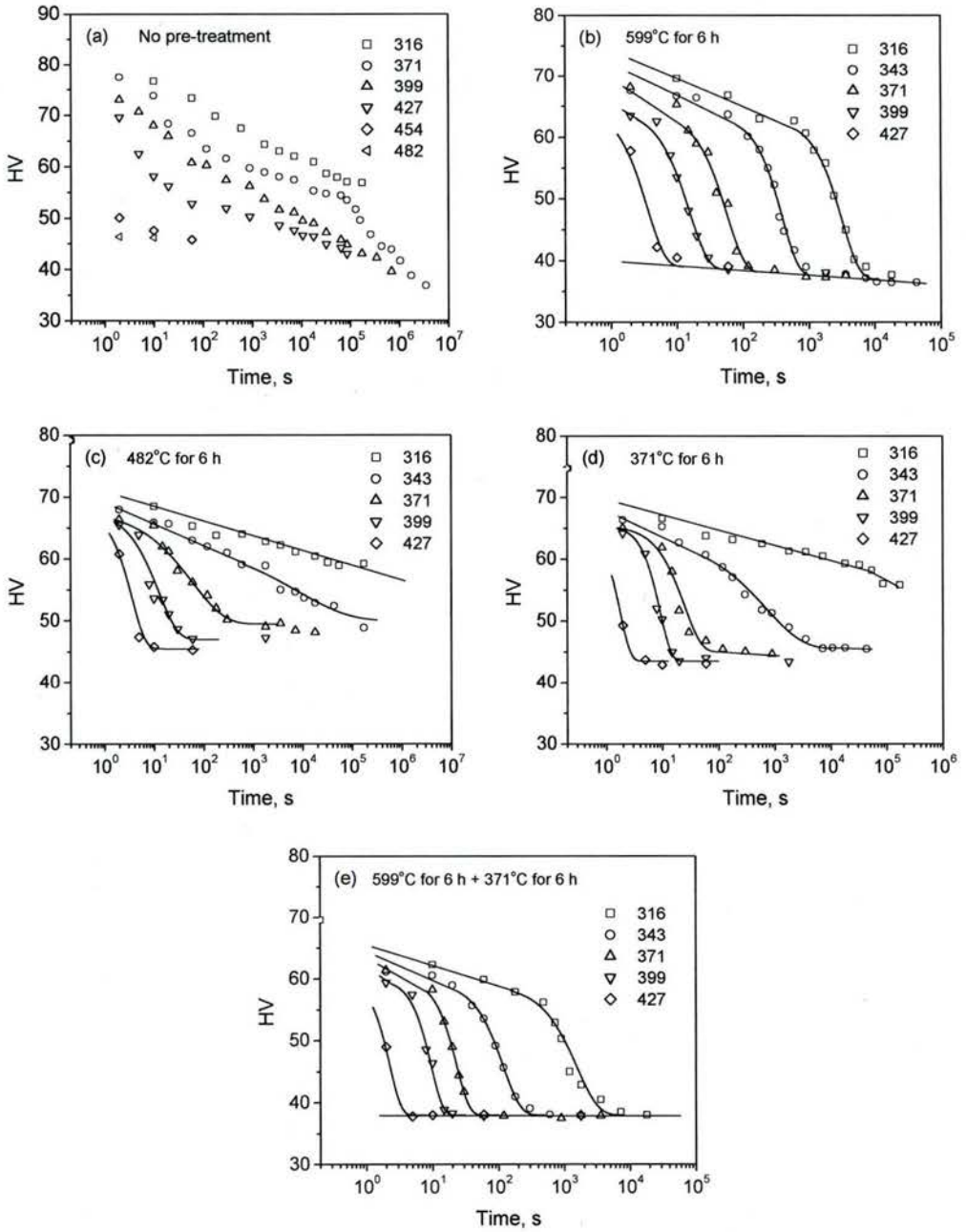

Fig. 12. Hardness as a function of annealing time at different temperatures for CC AA 3105 hot band (a) directly cold rolled to 75% reduction, or preheat treated at (b) 599°C for 6 h, (c) 482°C for 6 h, (d) 371°C for 6 h, and (e) 599°C for 6 h + 371°C for 6 h, and then cold rolled to 75% reduction. The hardness of these initial cold rolled sheets before annealing was measured to be 93, 83, 79, 75, and 70, respectively.

The pre-treatment prior to cold rolling affected not only the recrystallization of CC AA 3105 aluminum alloy, but also the hardness of cold rolled and fully recrystallized sheets. The hardness of the cold rolled sheets with different pre-treatments was given in the caption of Fig. 12. The hardness of directly cold rolled CC 3105 aluminum alloy was measured to be around 92.9. The hardness of cold rolled sheets decreased in the sequence of pre-treatment conditions A→B→D→F→G. The change in the hardness of cold rolled sheets is mainly caused by different degrees of solid solution strengthening. The pre-treatments prior to cold rolling also affected the hardness after complete recrystallization. After annealing at 427°C, the sample under the D condition possessed the highest hardness, while the hardness of the sample under the G condition was the lowest.

3.1.2. Recrystallized grains

Microstructure change during recrystallization has been extensively reported. The present work focuses mainly on the comparison of recrystallized grains. Figs. 13 to 17 show the grain structures of CC AA 3105 aluminum alloy with different preheat treatments after annealing at different temperatures. Under the A condition (Fig. 13), the deformed structure was almost fully recrystallized after annealing at 371°C for 40 days. The microstructure showed coarse elongated recrystallized grains. As the annealing temperature increased, the size of recrystallized grains decreased. At high temperatures, very fine elongated grains were obtained.

Under the B condition (Fig. 14), fine equiaxed recrystallized grains were observed at all annealing temperatures. The annealing temperature hardly affected the size of recrystallized grains.

Under the D condition (Fig. 15), the deformed structure was partially recrystallization after annealing at 343°C for 2 days, at 371°C for 2 h, and at 399°C for 1 min. However, based on the curves of hardness and time shown in Fig. 12(c), the hardness decreased to a low level value after annealing for a selected long time. The reason for the D materials not to reach complete recrystallization is undoubtedly attributed to the effect of the fine precipitates on recrystallization. After annealing at 427°C for 1 min and at 482°C for 10 s, the deformed structure was fully recrystallized.

Under the F condition (Fig. 16), the deformed structure was partially recrystallization after annealing at 343°C for 5 h, at 371°C for 15 min, and at 399°C for 1 min. Compared with the curves of hardness and time, it is seen that the relationship between microstructure and hardness was similar to that under the D condition. After annealing at 427°C for 1 min and at 482°C for 10 s, the deformed structure was fully recrystallized.

Under the G condition (Fig. 17), at 316°C, relatively coarse, slightly elongated recrystallized grains were observed. As the annealing temperature increased, the size of the recrystallized grains decreased and the recrystallized grains became gradually equiaxed. At high temperatures, a fine equiaxed grain structure was obtained. In comparison to the B condition, the recrystallized grains under the G condition were larger than those under the B condition at a given annealing temperature, indicating that the fine precipitates produced by the additional pre-treatment at 371°C increased the size of recrystallized grains.

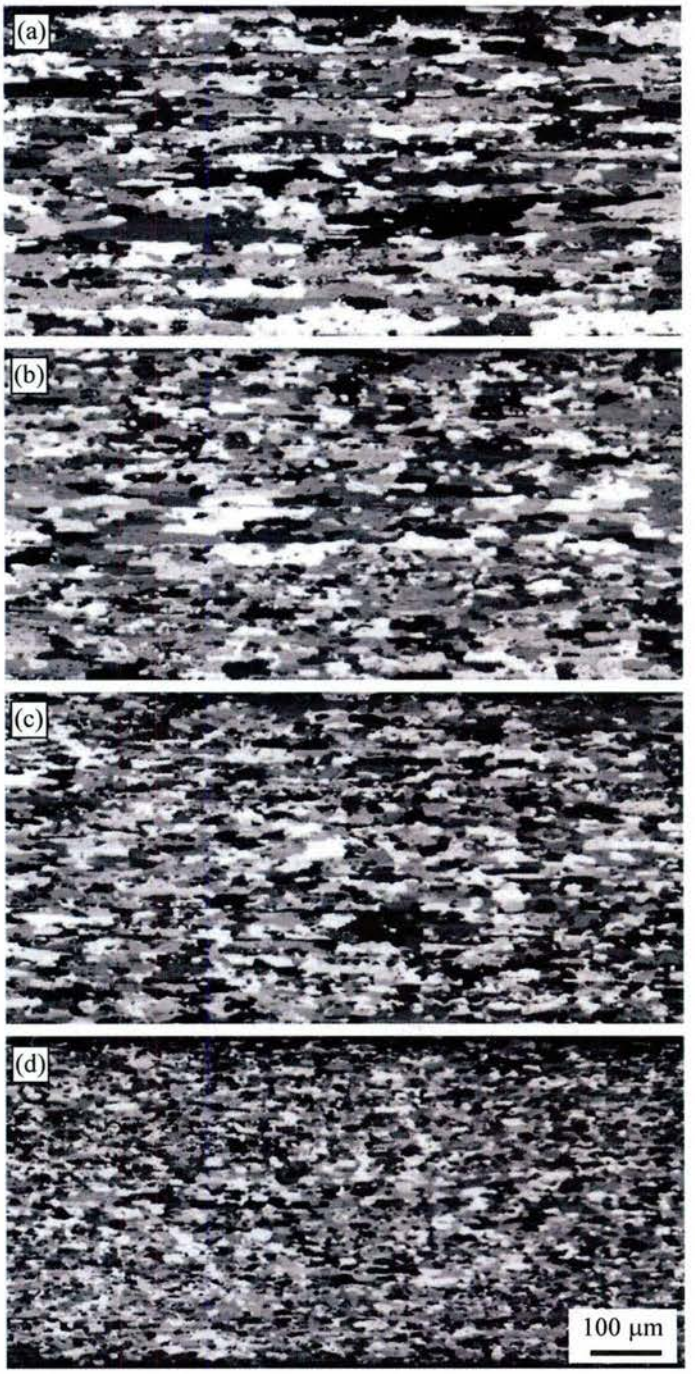

Fig. 13. Recrystallized grains of cold rolled AA 3105 aluminum alloy under the A condition after annealing at (a) 371°C for 40 days, (b) 399°C for 8 days, (c) 427°C for 9 h, and 482°C for 10 s.

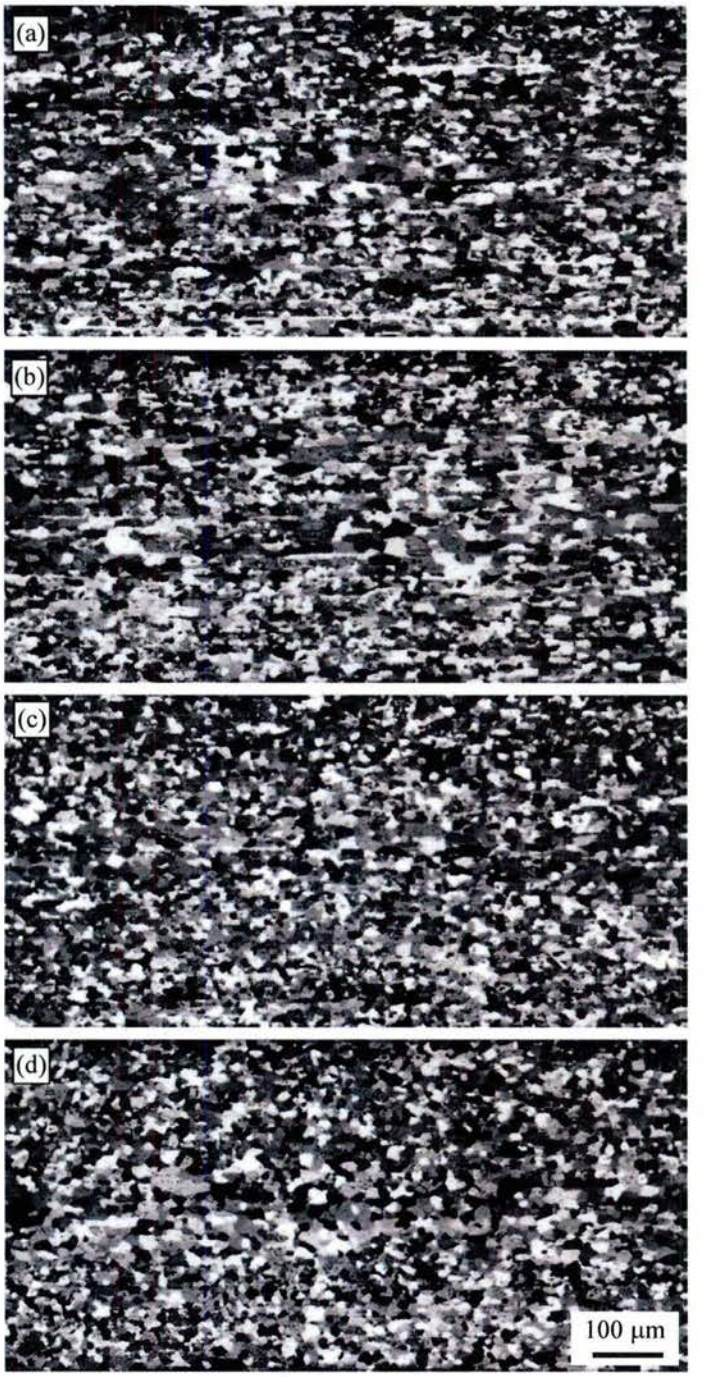

Fig. 14. Recrystallized grains of cold rolled AA 3105 aluminum alloy under the B condition after annealing at (a) 316°C for 5 h, (b) 371°C for 5 min, (c) 427°C for 10 s, and 482°C for 10 s.

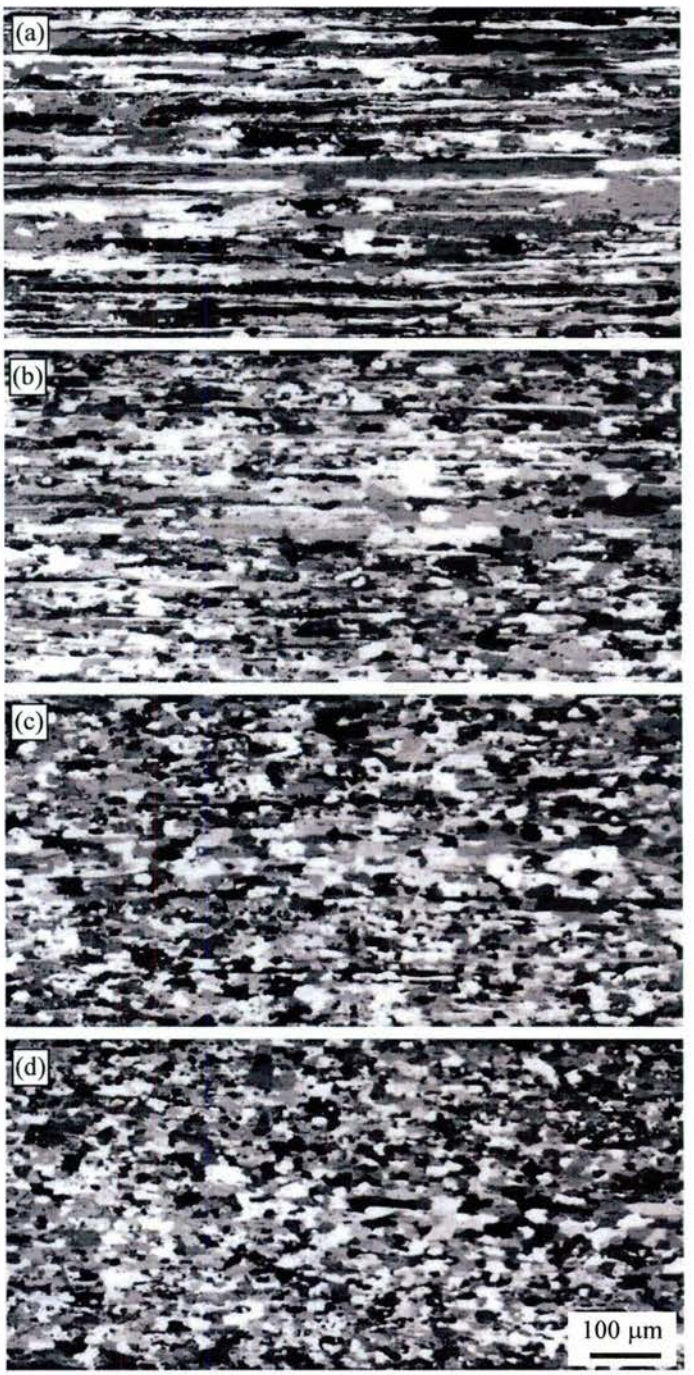

Fig. 15. Grain structure of cold rolled AA 3105 aluminum alloy under the D condition after annealing at (a) 343°C for 2 days, (b) 399°C for 1 min, (c) 427°C for 1 min, and (d) 482°C for 10 s.

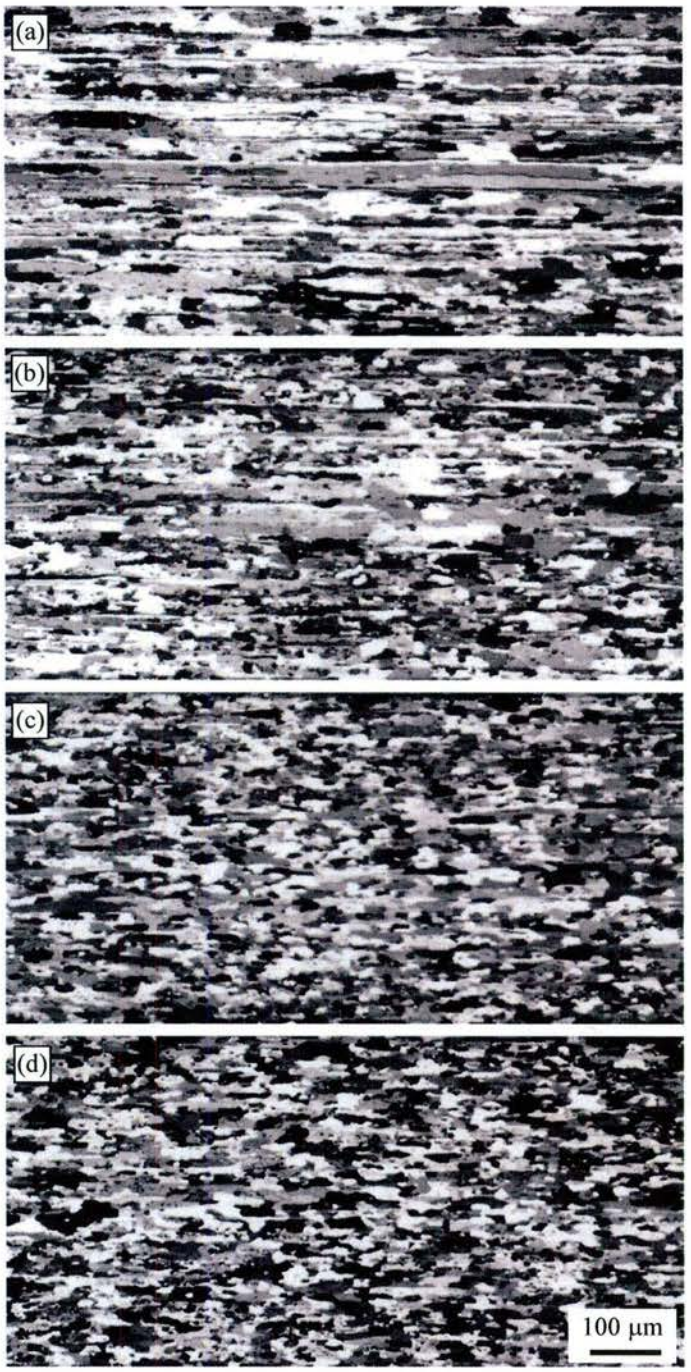

Fig. 16. Grain structure of cold rolled AA 3105 aluminum alloy under the F condition after annealing at (a) 343°C for 5 h, (b) 399°C for 1 min, (c) 427°C for 1 min, and (d) 482°C for 10 s.

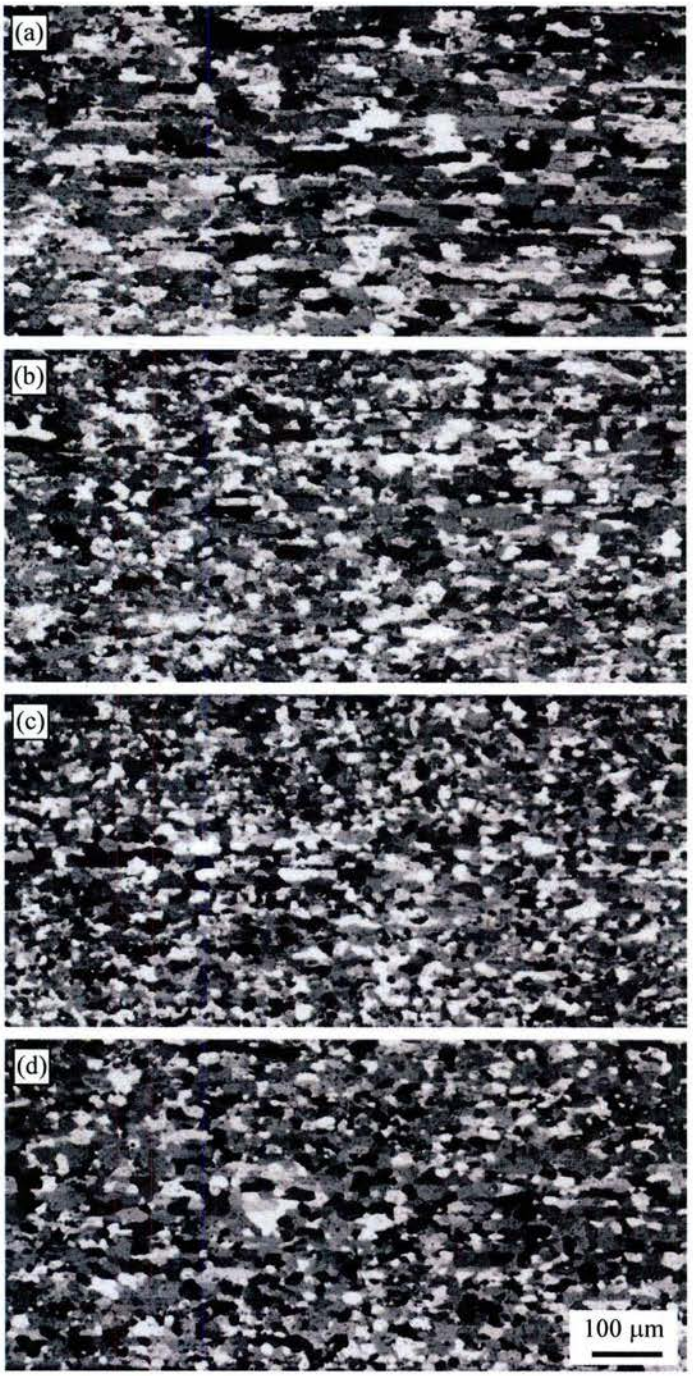

Fig. 17. Recrystallized grains of cold rolled AA 3105 aluminum alloy under the G condition after annealing at (a) 316°C for 2 h, (b) 371°C for 1 min, (c) 427°C for 10 s, and 482°C for 10 s.

3.1.3. Recrystallization kinetics

For CC AA 3105 aluminum alloy without pre-treatment (A condition), the hardness decreased gradually with increasing annealing time. Its recrystallization kinetics can not be determined by measurements of hardness. For this alloy with different pre-treatments, the recrystallized volume fraction $X(t)$ was estimated from the variation in hardness HV with annealing time t by:

$$X(t) = \frac{HV_{RV} - HV(t)}{HV_{RV} - HV_{RX}} \tag{3}$$

Here, HV_{RV} denotes the hardness after recovery prior to the onset of recrystallization, and HV_{RX} the hardness after complete recrystallization. The values of HV_{RV} and HV_{RX} were estimated from the hardness-time curves combined with the observation of microstructure, as listed in Table 5.

The recrystallized volume fraction as a function of annealing time is well described by the standard Johnson-Mehl-Avrami-Kolmogorov (JMAK) equation:

$$X(t) = 1 - \exp(-kt^n) \tag{4}$$

where k is a constant and n is the JMAK exponent. The $X(t)$ data can be plotted in a $\ln[-\ln(1-f)]$ *vs.* $\ln(t)$ format. The values of k and n were determined by fitting the experimental data into Equation (4). The results are also shown in Table 5. Under the B condition, the n value was estimated to be about 1.7, and it did not vary with annealing temperature. Under the D and F conditions, the n value increased with increasing annealing temperature. At a given annealing temperature, the n value under the D condition was smaller than that under the F condition. Under the G condition, the n value at 316°C was estimated to be 1.3, and it increased with increasing annealing temperature.

Table 5. Values of k and n for recrystallization kinetics of cold rolled AA 3105 aluminum alloy with different pre-treatments.

Code	Heat treatment	Temperature, °C	HV_{RV}	HV_{RX}	k	n
B	599°C, 6 h	316	63.0	37.0	$1.4\cdot10^{-6}$	1.7
		343	63.5	37.5	$2.3\cdot10^{-5}$	1.8
		371	64.0	38.0	$1.7\cdot10^{-3}$	1.6
		399	64.5	38.5	$1.6\cdot10^{-2}$	1.5
D	482°C, 6 h	343	63.0	50.0	$2.4\cdot10^{-2}$	0.41
		371	68.0	49.5	$6.7\cdot10^{-2}$	0.66
		399	68.0	47.0	$5.9\cdot10^{-2}$	1.13
F	371°C, 6 h	343	63.5	45.5	$1.4\cdot10^{-2}$	0.65
		371	65.5	45.0	$1.0\cdot10^{-2}$	1.42
		399	65.5	43.5	$8.0\cdot10^{-3}$	2.18
G	593°C, 6 h and 371°C, 6 h	316	59.0	38.0	$5.4\cdot10^{-5}$	1.3
		343	59.5	38.0	$3.8\cdot10^{-4}$	1.6
		371	60	38.0	$8.2\cdot10^{-4}$	2.2
		399	60	38.0	$4.3\cdot10^{-3}$	2.4

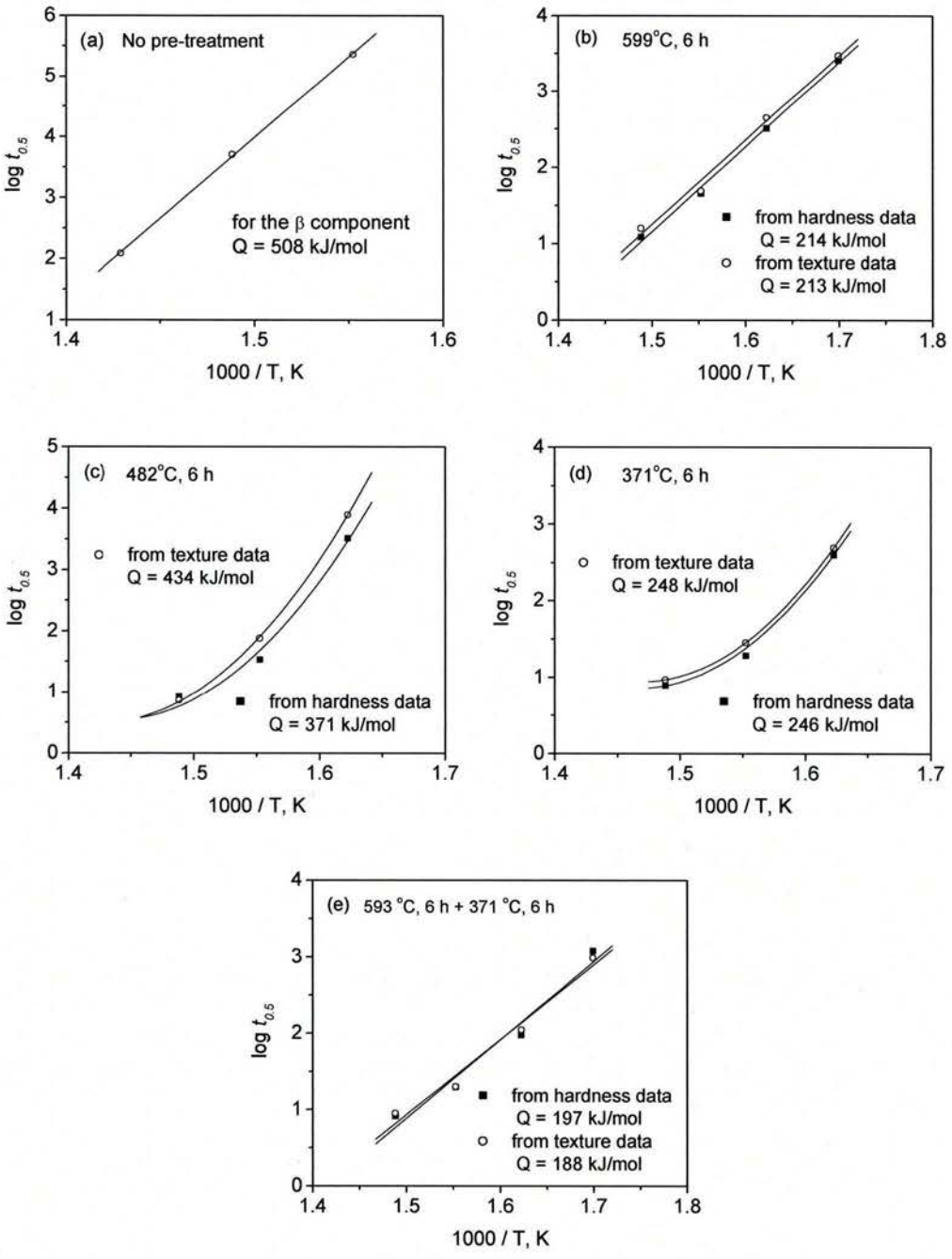

Fig. 18. log $t_{0.5}$ versus inverse temperature plots used for the apparent activation energy for recrystallization of CC AA 3105 aluminum alloy. (a) no pre-treatment, (b) 599°C for 6 h, (c) 482°C for 6 h, (d) 371°C for 6 h, and (e) 599°C for 6 h + 371°C for 6 h.

The time to 50% recrystallization ($t_{0.5}$), which was derived from equation (4), is related to the temperature and the activation energy in an Arrhenius-type representation:

$$t_{0.5} = \tau_0 \exp(Q_{RX} / RT) \tag{5}$$

Here, τ_o is a constant, Q_{RX} is the apparent activation energy for recrystallization, R is the universal gas constant, and T is the annealing temperature in Kelvin. Taking logarithms of both sides in Equation (5), $ln\ t_{0.5}$ against $1/T$ is plotted in Fig. 18. Under the B and G conditions, straight lines are expected. The apparent activation energy for recrystallization of CC AA 3105 aluminum alloy was estimated to be 214 and 197 kJ/mole under the B and G conditions, respectively. Under the D and F conditions, the relationship between $ln\ t_{0.5}$ and $1/T$ shows polynomial curves, which indicate that the apparent activation energy for recrystallization increases with decreasing annealing temperature. If it is assumed that the relationship between $ln\ t_{0.5}$ and $1/T$ follows a straight line, then the average apparent activation energy for recrystallization under the D and F conditions was 371 and 246 kJ/mol, respectively. The apparent activation energy for recrystallization under the A condition can not be determined by measurements of hardness. The apparent activation energy for recrystallization, which was determined from texture data, is given in Section 3.2.3.

3.2. Global texture changes

3.2.1. Texture of cold rolled samples

Fig. 19 shows the texture of cold rolled CC AA 3105 aluminum alloy with different pre-treatments. During cold rolling all initial orientations were rotated to the stable end orientations, i.e. the β fiber component. The texture evolution during rolling depended strongly on the initial texture. Since the hot band and hot band preheated at 371°C for 6 h possessed the β fiber rolling texture, further cold rolling increased the strength of the β fiber rolling texture. The hot band that was preheat treated at 599°C for 6 h, 482°C for 6 h, and 599°C for 6 h + 371°C for 6 h exhibited weak recrystallization textures. After 75% cold rolling, the β fiber rolling texture was weaker than that formed in the directly cold rolled hot band.

3.2.2. Evolution of recrystallization texture

During annealing of the cold rolled samples, recovery and recrystallization took place. The β fiber rolling texture was converted into recrystallization textures. Fig. 20 shows the texture evolution of cold rolled AA 3105 aluminum alloy under the A condition during isothermal annealing at different temperatures. It is noted that there was no significant texture change during recovery of the cold rolled samples. The evolution of recrystallization texture depended strongly on the annealing temperature. At 371°C, the strength of the β fiber rolling texture started to decrease after 1 min. The intensities of orientations along the β fiber decreased with increasing annealing time, whereas the intensity of the P orientation increased. After complete recrystallization at 40 days, the recrystallization texture was characterized by a strong P component. At 399°C, the strength of the β fiber rolling texture started to decrease after 2 s. The intensities of orientations along the β fiber decreased with increasing annealing time, whereas the intensity of the P orientation increased. After complete recrystallization at 8 days, the intensity of

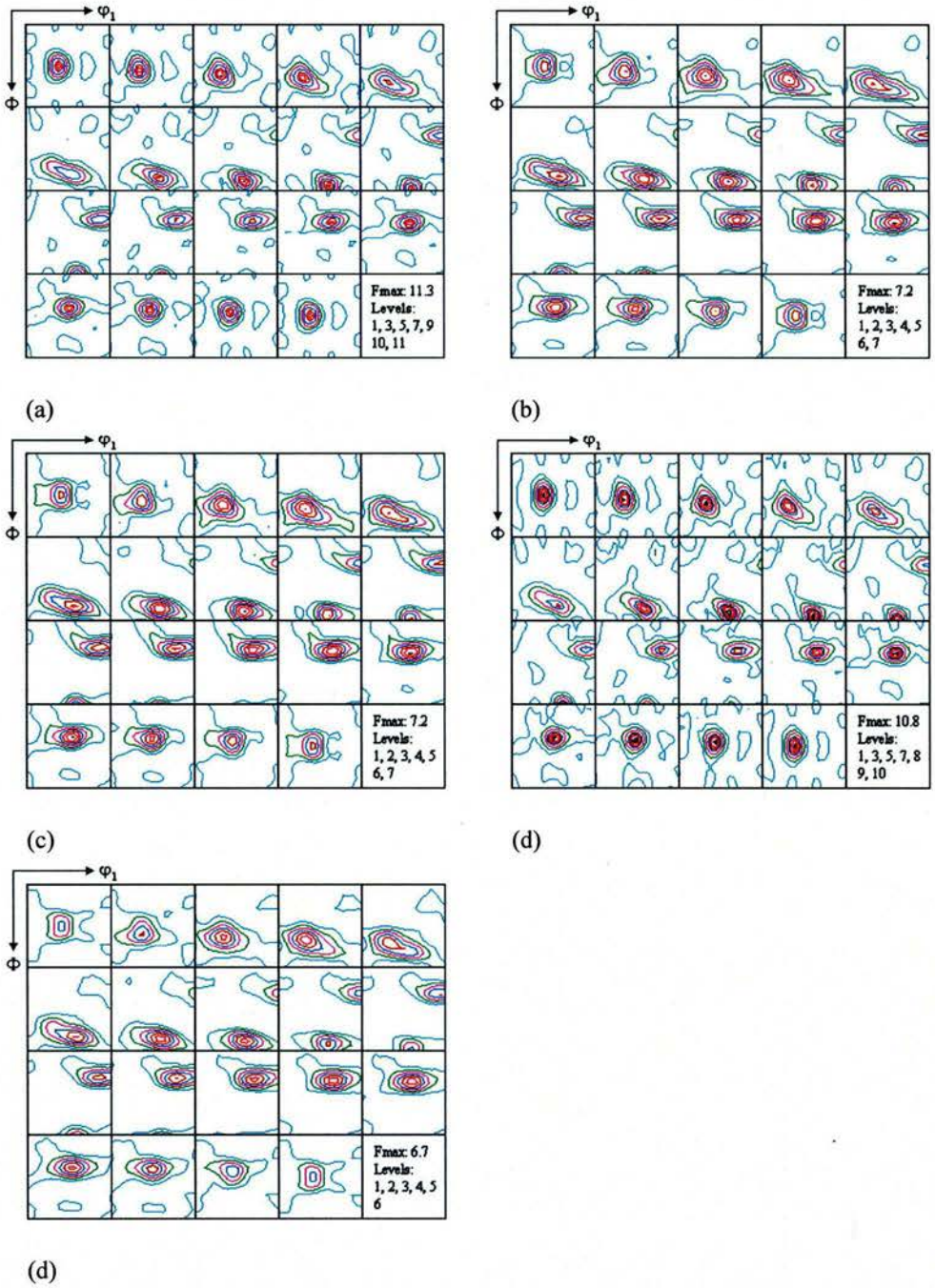

Fig. 19. ODFs of cold rolled CC AA 3105 aluminum alloy (a) without pre-treatment and with the pre-treatments of (b) 599°C for 6 h, (c) 482°C for 6 h, (d) 371°C for 6 h, and (e) 599°C for 6 h + 371°C for 6 h.

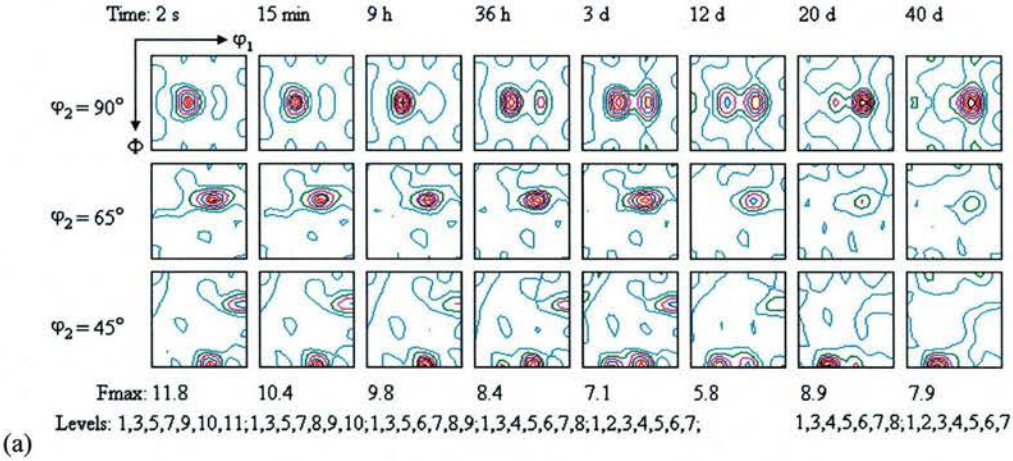

(a)

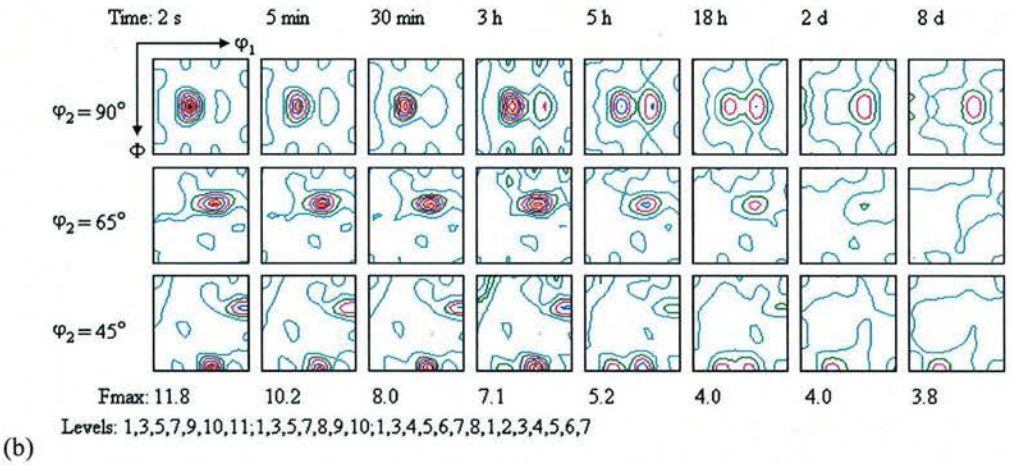

(b)

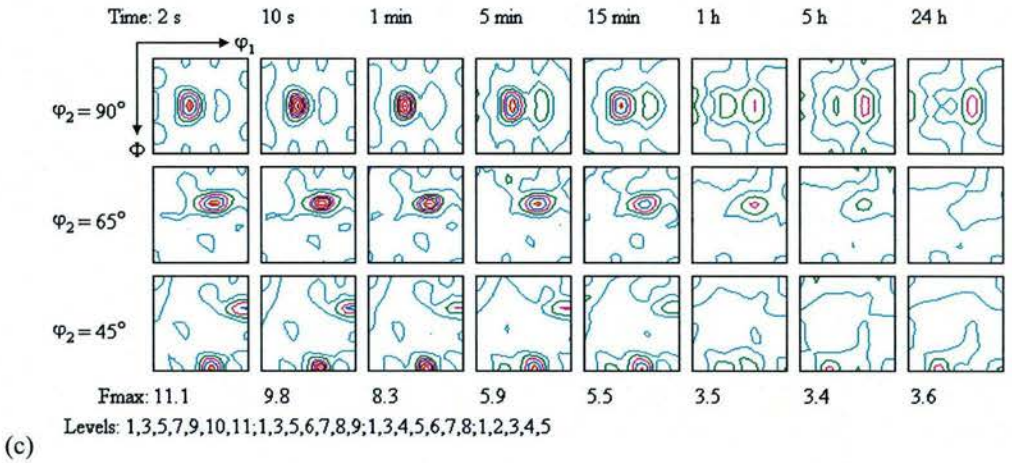

(c)

Fig. 20. Texture evolution of cold rolled AA 3105 aluminum alloy under the A condition during isothermal annealing at (a) 371, (b) 399, and (c) 427°C.

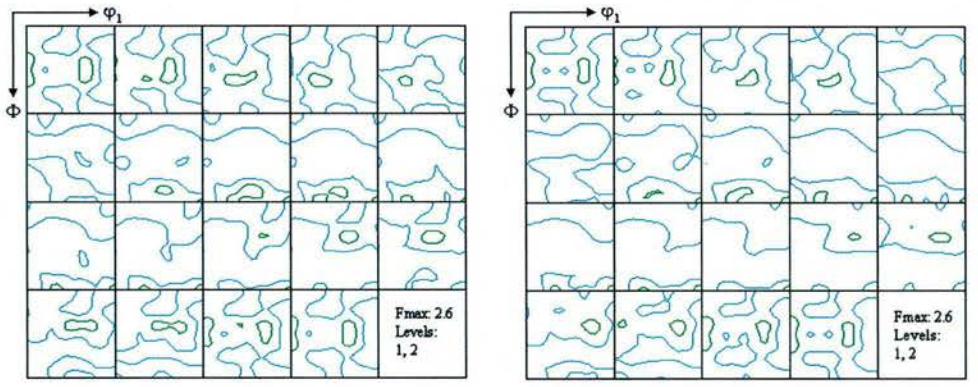

(a) (b)

Fig. 21. Recrystallization texture of cold rolled AA 3105 aluminum alloy under the A condition after annealing at (a) 454°C for 1 min and (b) 482°C for 10 s.

the P orientation was lower than that at 371°C. Fig. 21 shows the recrystallization texture of AA 3105 aluminum alloy under the A condition after annealing at 454 and 482°C. It is seen that the β fiber rolling texture disappeared after a short incubation time. The resulting recrystallization texture consisted of a weak P component.

Fig. 22 shows the texture evolution of cold rolled AA 3105 aluminum alloy with a pre-treatment of the B condition during isothermal annealing at different temperatures. Fig. 23 shows the recrystallization texture after annealing at 427, 454 and 482°C. It is noted that the texture evolution of the alloy with this pre-treatment during annealing was completely different from that of the alloy without pre-treatment. At 316°C, the strength of the β fiber rolling texture started to decrease after 10 min. The intensities of orientations along the β fiber decreased with increasing annealing time, whereas the intensity of the cube orientation increased. After complete recrystallization, the recrystallization texture was characterized by a weak cube component. As the annealing temperature increased, recrystallization took place and finished at a shorter time. The annealing temperature did not affect the cube recrystallization texture of CC AA 3105 aluminum alloy under the B condition, but the strength of the R texture decreased slightly with increasing annealing temperature.

Fig. 24 shows the texture evolution of cold rolled AA 3105 aluminum alloy with a pre-treatment of the D condition during isothermal annealing at different temperatures. Fig. 25 shows the recrystallization texture after annealing at 427, 454 and 482°C. At 343°C, the strength of the β fiber rolling texture started to decrease after 5 min. The intensities of orientations along the β fiber decreased with increasing annealing time. After annealing for 2 days, the resulting texture was characterized by a major R component and a minor cube component. As the annealing temperature increased, recrystallization took place at a shorter time. The annealing temperature strongly affected the R recrystallization texture of CC AA 3105 aluminum alloy under the D condition. The strength of the R texture decreased with increasing annealing temperature. At high temperatures, the recrystallization texture consisted of a weak cube component.

Fig. 26 shows the texture evolution of cold rolled AA 3105 aluminum alloy with a pre-treatment of the F condition during isothermal annealing at different temperatures. Fig. 27 shows

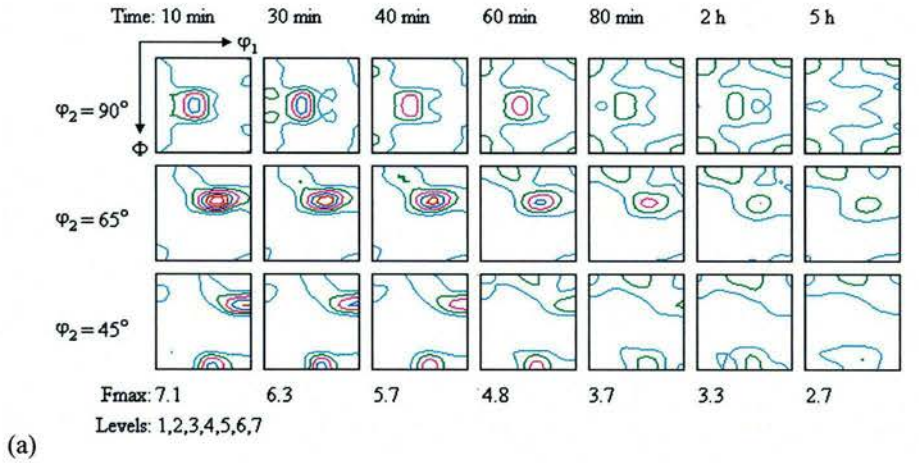

(a)

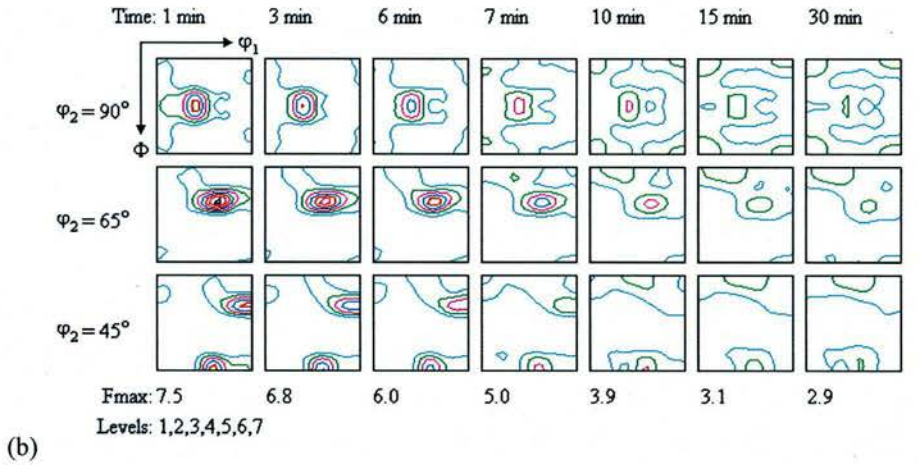

(b)

Fig. 22. Texture evolution of cold rolled AA 3105 aluminum alloy under the B condition during isothermal annealing at (a) 316, (b) 343, (c) 371, and (d) 399°C.

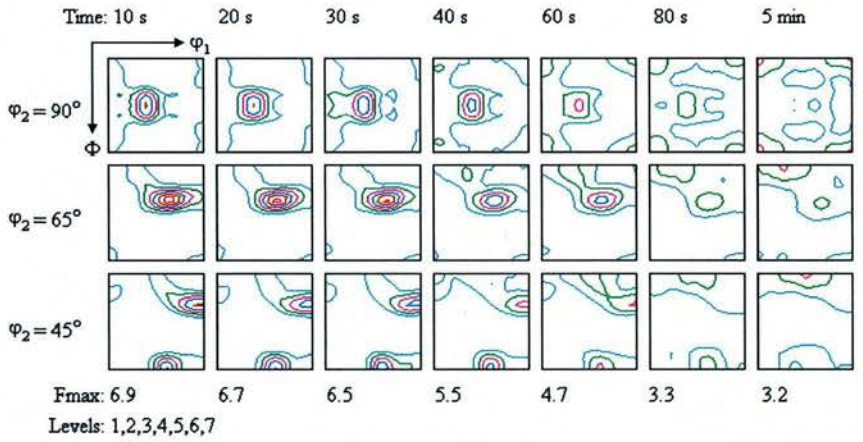

(c)

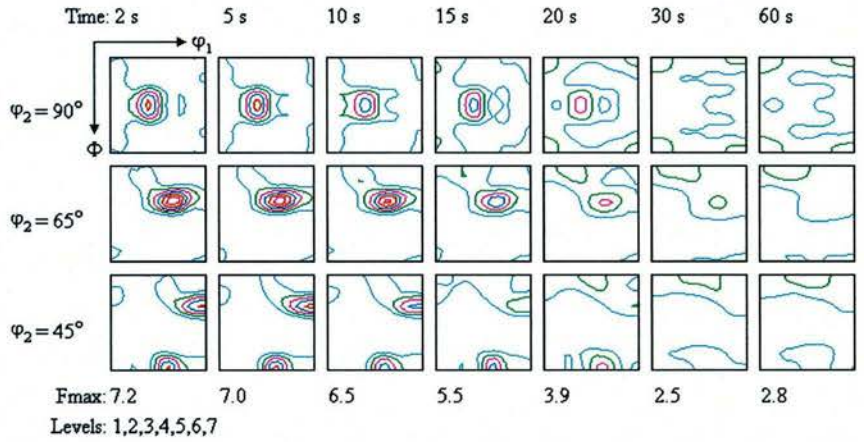

(d)

Fig. 22. Continuous.

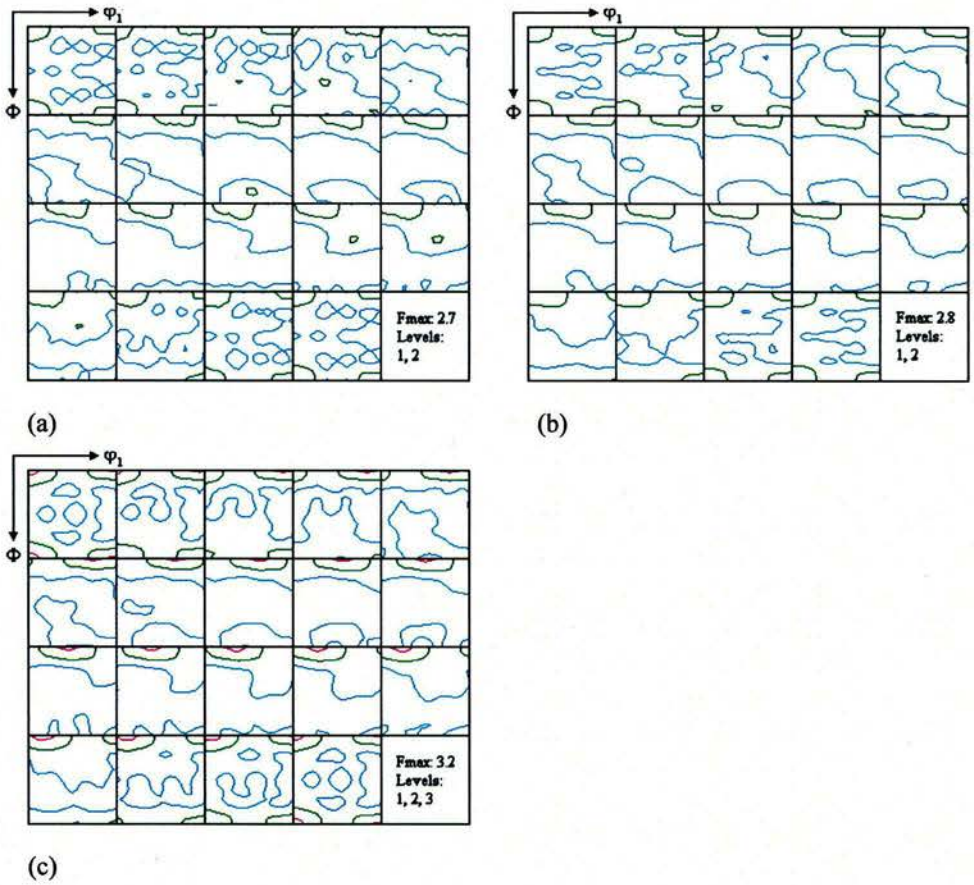

Fig. 23. Recrystallization texture of cold rolled AA 3105 aluminum alloy under the B condition after annealing at (a) 427, (b) 454, and (c) 482°C for 10 s.

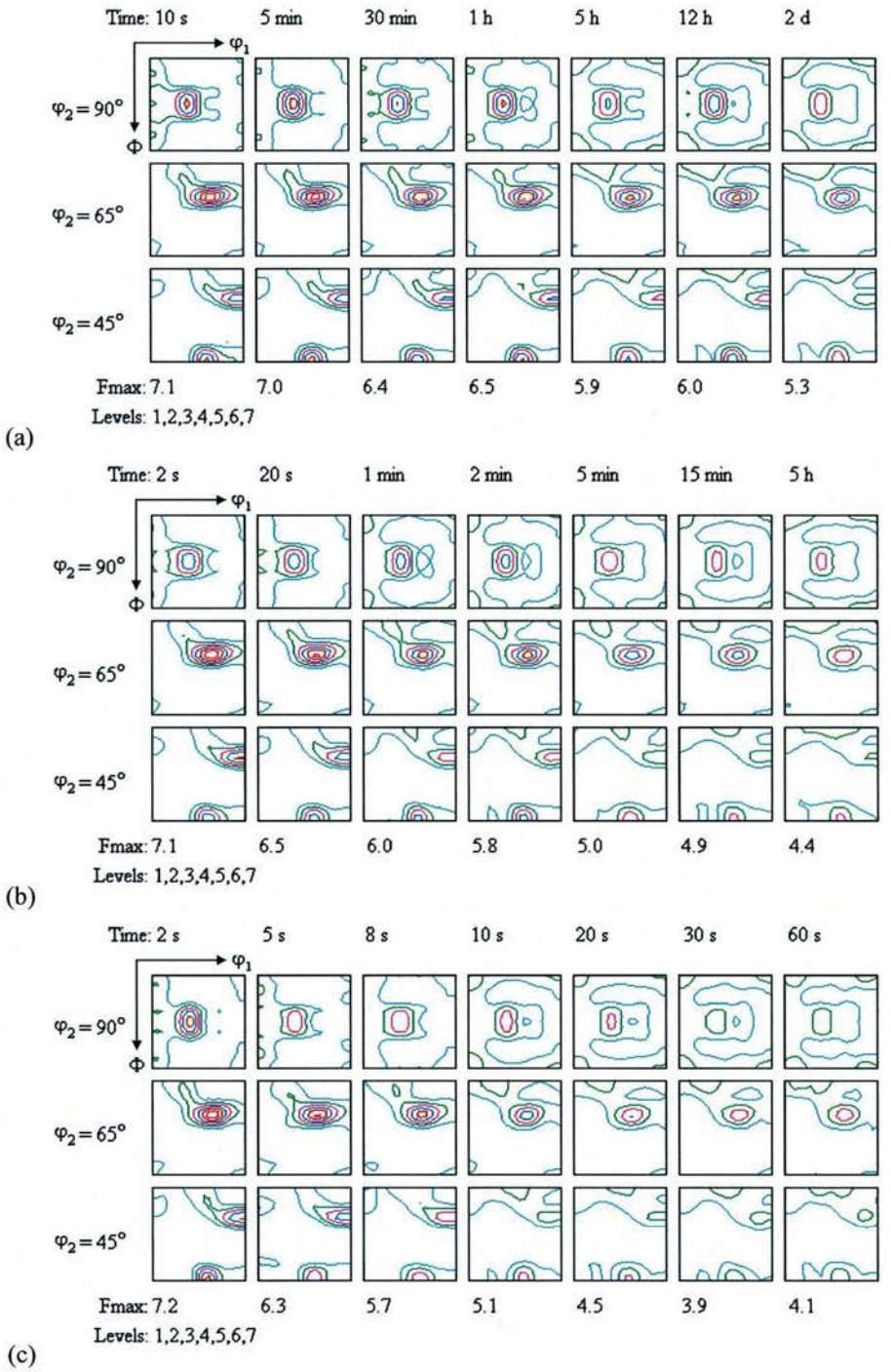

Fig. 24. Texture evolution of cold rolled AA 3105 aluminum alloy under the D condition during isothermal annealing at (a) 343, (b) 371, and (d) 399°C.

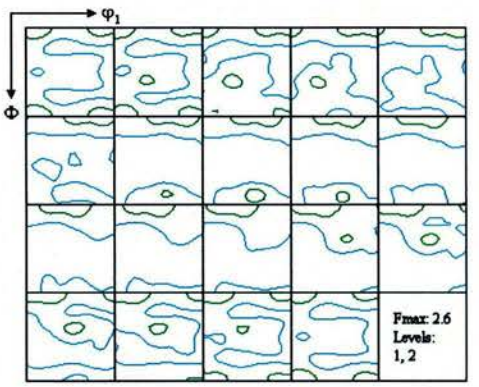

(a) 427°C, 10s

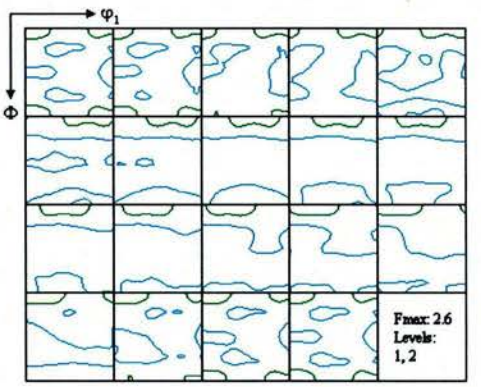

(b) 454°C, 10 s

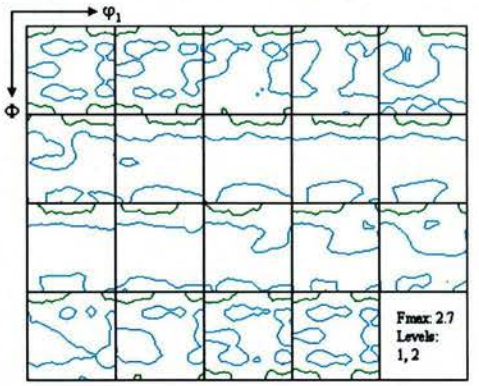

(c) 482°C, 10s

Fig. 25. Recrystallization texture of cold rolled CC AA 3105 aluminum alloy under the D condition after annealing at (a) 427, (b) 454, and (c) 482°C for 10 s.

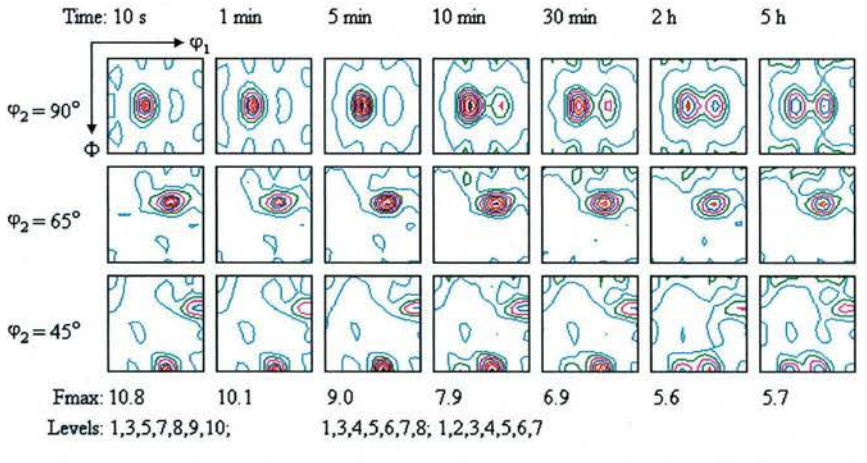

(a)

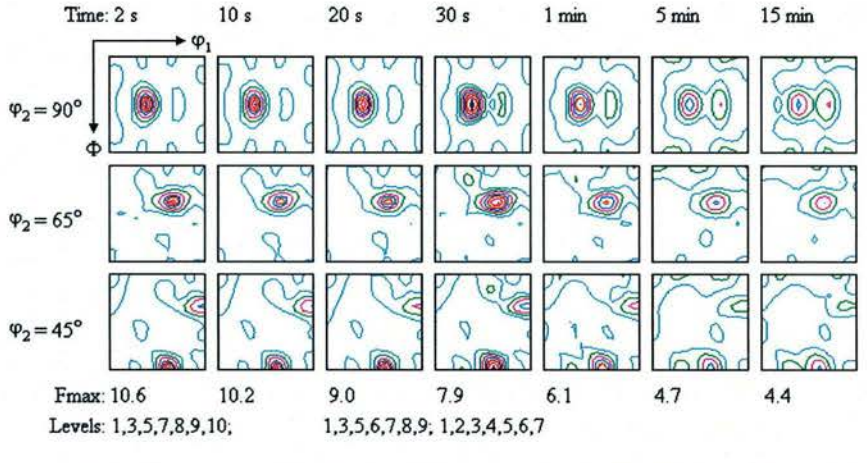

(b)

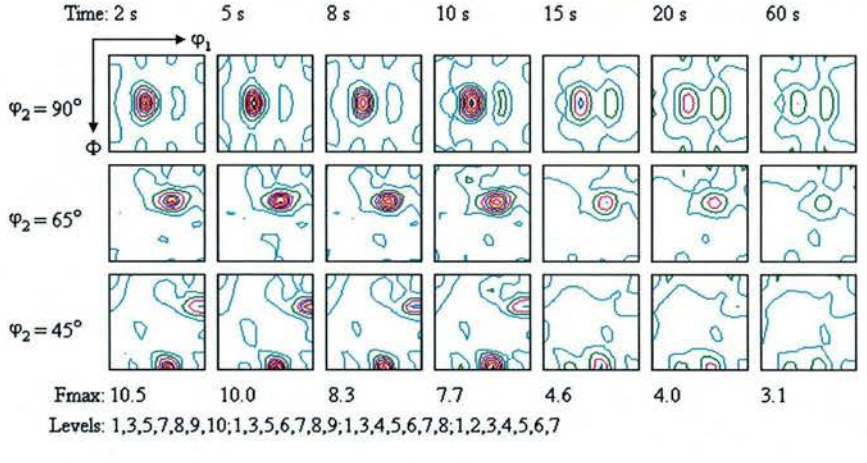

(c)

Fig. 26. Texture evolution of cold rolled AA 3105 aluminum alloy under the F condition during isothermal annealing at (a) 343, (b) 371, and (c) 399°C.

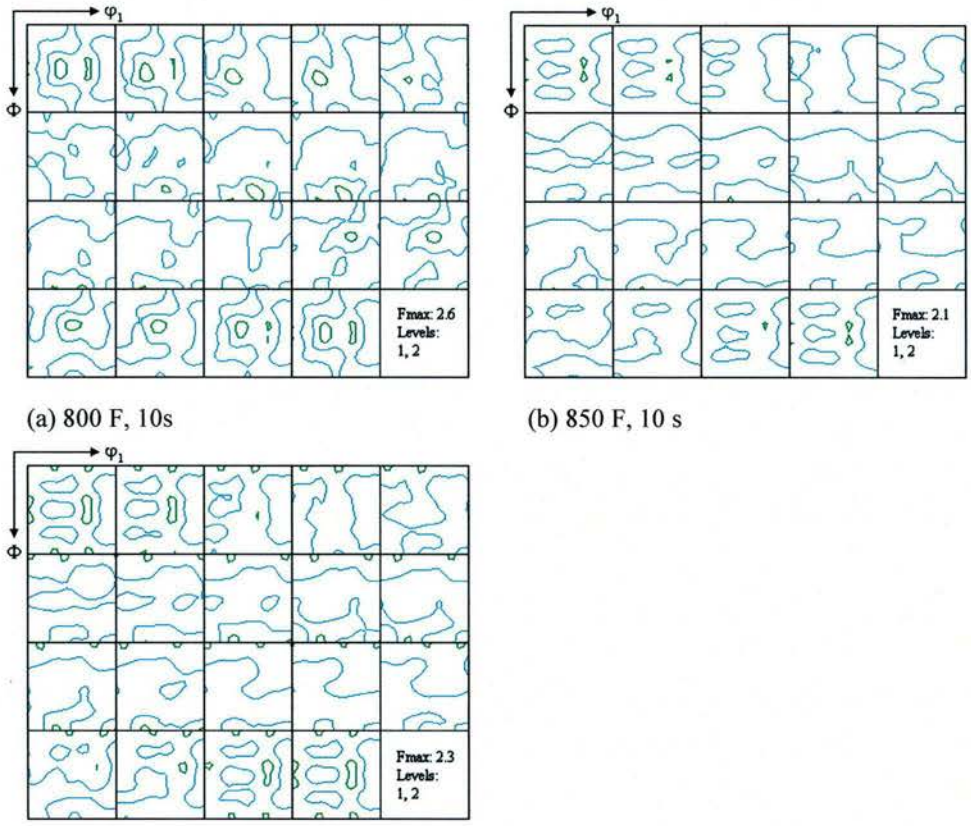

(a) 800 F, 10s

(b) 850 F, 10 s

(c) 900 F, 10s

Fig. 27. Recrystallization texture of cold rolled CC AA 3105 aluminum alloy under the F condition after annealing at (a) 427, (b) 454, and (c) 482°C for 10 s.

the recrystallization texture after annealing at 427, 454 and 482°C. At 343°C, the strength of the β fiber rolling texture started to decrease after 20 s. The intensities of orientations along the β fiber decreased with increasing annealing time, whereas the intensity of the P orientation increased. After annealing for 5 h, i.e. when the hardness reached a low level value, the resulting texture was characterized by strong R and P components. The annealing temperature strongly affected the recrystallization texture of CC AA 3105 aluminum alloy under the F condition. The strength of the R and P textures decreased with increasing annealing temperature. At high temperatures, the recrystallization texture consisted of a very weak P component.

Fig. 28 shows the texture evolution of cold rolled AA 3105 aluminum alloy with a pre-treatment of the G condition during isothermal annealing at different temperatures. Fig. 29 shows the recrystallization texture after annealing at 399, 427, 454 and 482°C. It is noted that the texture evolution of the alloy under the G condition during annealing was similar to that under the B condition. At 316°C, the strength of the β fiber rolling texture started to decrease after 2 min. The

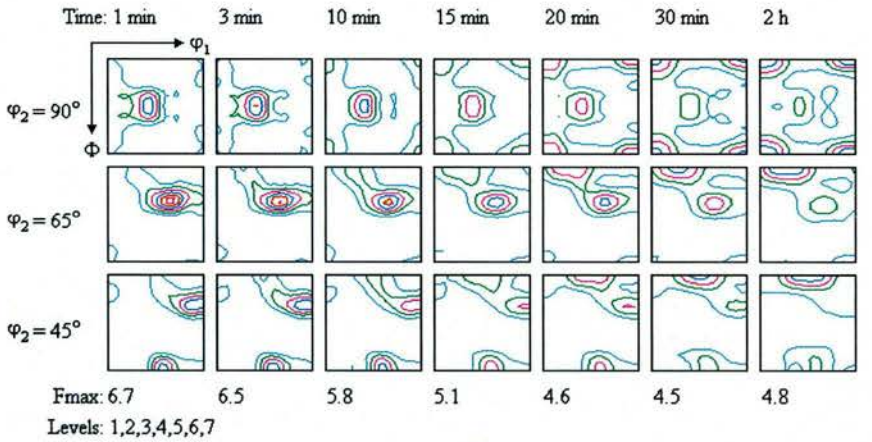

(a)

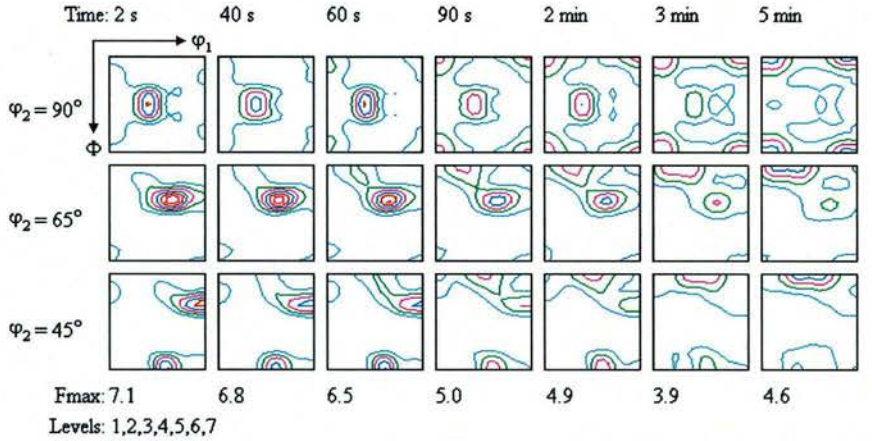

(b)

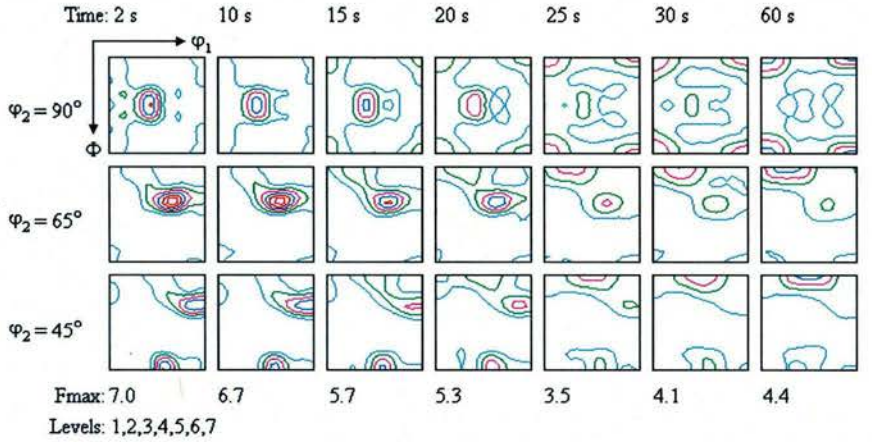

(c)

Fig. 28. Texture evolution of cold rolled AA 3105 aluminum alloy under the G condition during isothermal annealing at (a) 316, (b) 343, and (c) 371°C.

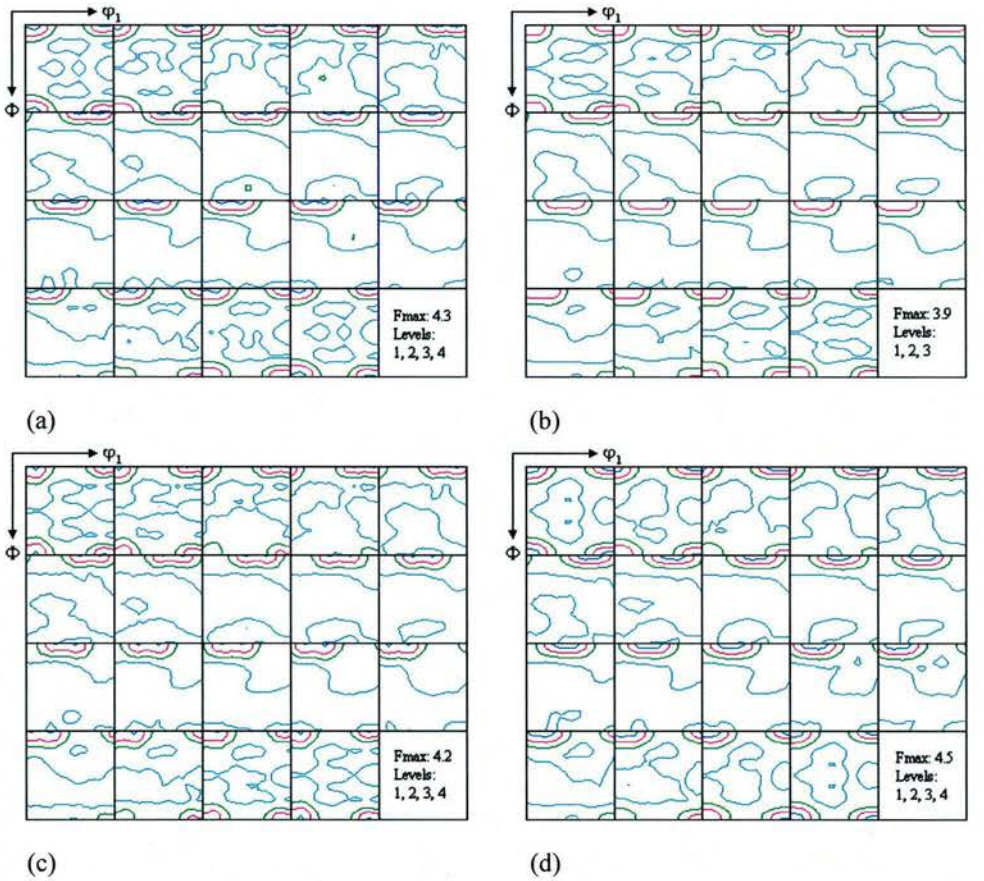

Fig. 29. Recrystallization texture of cold rolled AA 3105 aluminum alloy under the G condition after annealing at (a) 399°C for 20 s, (b) 427°C for 10 s, (c) 454°C for 10 s, and (d) 482°C for 10 s.

intensities of orientations along the β fiber decreased with increasing annealing time, whereas the intensity of the cube orientation increased. After complete recrystallization, the recrystallization texture was characterized by a major cube component and a minor R component. The annealing temperature hardly affected the cube recrystallization texture of CC AA 3105 aluminum alloy under the G condition, but the strength of the R texture decreased slightly with increasing annealing temperature. In contrast to the recrystallization texture under the B condition, the cube recrystallization texture under the G condition was stronger, indicating that the additional heat treatment at 371°C stimulates the formation of the cube component.

3.2.3. Quantitative analysis of recrystallization texture evolution

In order to give a more complete survey of the evolution of recrystallization texture during annealing, the texture volume fractions were calculated by an improved integration method, as shown in Tables 6 to 10. Figs. 30 to 34 depict the texture volume fractions as a function of annealing time at different temperatures for cold rolled CC AA 3105 aluminum alloy with different pre-treatments. It is clear that the texture volume fractions only slightly varied with the annealing time during recovery and after complete recrystallization. Significant changes in the texture volume fractions occurred during recrystallization. Fig. 35 shows the effect of annealing temperature on recrystallization textures, where the ratio ($M_i/M_{i\text{-}random}$) of the volume fraction of the texture component (M_i) to that under a perfectly random condition ($M_{i\text{-}random}$) is plotted as a function of annealing temperature. The volume fractions of the cube, r-cube, Goss, r-Goss, β fiber/R, P and remainder components are 5.41, 5.64, 6.45, 9.09, 16.90, 5.03 and 51.47 % in a perfectly random sample, respectively.

For the CC AA 3105 aluminum alloy under the A condition, it is found that the texture evolution during annealing depended on the annealing temperature. At low temperatures, the volume fraction of the β fiber component decreased with increasing annealing time, whereas the volume fractions of the P, r-cube and remainder components increased. After complete recrystallization, the recrystallization texture consisted of a strong P component (Fig. 35(a)). At high temperatures, the volume fraction of the β fiber component decreased with increasing annealing time, but the volume fraction of the P component only slightly increased. After complete recrystallization, the recrystallization texture consisted of a weak P component. The volume fractions of the cube and r-Goss components hardly changed with increasing annealing time. The annealing temperature strongly affected the recrystallization texture under the A condition. As the annealing temperature increased, the strength of the P component decreased markedly, whereas the strengths of the cube, Goss, and R components increased slightly. In addition, it is interesting to note that the r-cube component was not comparable to the P component, and did not increase with decreasing annealing temperature. This means that the formation of the P oriented grains does not necessarily accompany the r-cube oriented grains.

For the CC AA 3105 aluminum alloy under the B condition, the recrystallization texture was mainly characterized by the cube component. As the annealing temperature increased, the strength of the R component decreased slightly, whereas the strength of the r-cube component increased slightly. The strengths of the other components hardly varied with the annealing temperature. During recrystallization, the volume fractions of the Goss and β fiber components decreased, whereas the volume fractions of the cube, r-cube and remainder components increased. The volume fraction of the r-Goss component changed slightly.

For the CC AA 3105 aluminum alloy under the D condition, the volume fraction of the β fiber component decreased during recrystallization, whereas the volume fractions of the r-cube and remainder components increased. The recrystallization texture depended strongly on the annealing temperature. At low temperatures the recrystallization texture consisted of a major R component and a minor cube component. As the annealing temperature increased, the strength of the R component decreased markedly, whereas the strengths of the r-cube, r-Goss and remainder components increased. At high temperatures the recrystallization texture consisted of a weak cube component.

For the CC AA 3105 aluminum alloy under the F condition, the volume fraction of the β fiber component decreased during recrystallization, whereas the volume fractions of the r-cube, P and remainder components increased. The recrystallization texture depended strongly on the

Table 6. Texture volume fractions for CC AA 3105 hot band (A condition) cold rolled to 75% reduction, and then annealed at different temperatures for different times.

Temperature (°C)	Time	Texture volume fraction (%)						
		cube	r-cube	Goss	r-Goss	β /R	P	remainder
Cold rolled		5.1	-0.6	11.6	4.5	68.8	4.6	6.1
371	2 s	5.3	-1.4	12.6	5.1	68.8	4.3	5.2
	1 min	5.7	-0.7	11.2	5.5	65.6	4.5	8.2
	5 min	5.6	0.1	10.9	3.6	64.1	4.7	11.0
	15 min	5.5	0.3	10.7	5.0	62.4	5.6	10.6
	1 h	6.1	0.7	10.1	3.9	59.7	5.4	14.1
	9 h	5.8	2.3	8.8	3.8	55.2	7.2	16.8
	36 h	5.6	2.7	8.9	4.2	48.9	10.3	19.4
	44 h	4.8	2.4	10.1	5.8	45.8	11.1	20.0
	3 days	4.9	3.2	9.0	5.1	43.3	12.8	21.8
	8 days	3.6	4.2	8.1	4.9	38.5	13.9	25.8
	12 days	4.4	5.0	7.8	5.3	33.0	14.4	30.0
	20 days	4.4	5.3	8.0	5.9	30.4	17.7	28.2
	40 days	5.5	5.9	7.2	6.9	20.3	17.4	36.8
399	2 s	5.2	-0.4	11.5	3.8	68.6	4.1	7.2
	10 s	6.1	-0.5	11.1	3.7	66.5	4.6	8.5
	1 min	6.1	0.8	10.9	4.7	58.0	5.7	13.8
	5 min	5.4	1.3	10.4	4.1	59.0	6.3	13.5
	30 min	5.9	2.4	9.9	4.7	48.6	8.0	20.5
	1 h	6.0	2.4	9.9	4.5	49.4	8.1	19.6
	3 h	6.2	3.6	8.6	4.6	43.8	8.6	24.6
	5 h	5.5	4.8	8.3	5.3	32.8	11.1	32.3
	9 h	6.0	5.6	8.0	5.4	28.0	10.8	36.1
	18 h	5.3	5.8	7.5	5.2	28.6	11.3	36.3
	1 day	6.2	6.1	7.8	4.7	24.5	11.9	38.9
	2 days	5.9	6.2	7.1	5.3	22.0	11.5	42.0
	4 days	5.6	6.4	8.2	6.3	19.1	11.0	43.4
	8 days	6.5	6.7	7.3	6.5	17.9	11.3	43.9
427	2 s	5.1	-0.3	10.8	4.7	66.0	4.2	9.5
	10 s	5.9	1.0	10.5	3.7	58.2	5.7	14.9
	1 min	6.0	3.2	9.3	4.3	46.2	7.7	23.4
	5 min	6.6	4.1	9.0	4.7	38.1	8.4	29.0
	15 min	6.0	4.6	8.8	4.3	34.7	8.6	33.1
	1 h	6.4	5.8	8.3	4.9	26.5	9.7	38.4
	3 h	5.5	6.7	8.2	5.1	21.3	10.3	43.0
	5 h	6.0	6.8	7.5	6.1	22.5	10.2	41.0
	9 h	6.3	6.6	8.1	5.7	21.3	9.5	42.5
	24 h	6.1	7.0	7.9	5.5	18.8	10.5	44.2
454	2 s	6.7	1.8	10.1	5.0	53.0	6.0	17.4
	10 s	6.5	5.4	9.0	5.2	26.3	9.2	38.4
	1 min	6.9	6.0	8.9	5.6	22.8	8.5	41.3
482	2 s	7.1	6.1	9.1	5.8	21.0	8.1	42.8
	10 s	6.2	6.4	9.1	6.0	22.1	8.2	42.0

Table 7. Texture volume fractions for CC AA 3105 hot band annealed at 599°C for 6 h (B condition), cold rolled to 75% reduction, and then annealed at different temperatures for different times.

Temperature (°C)	Time	Texture volume fraction (%)						
		cube	r-cube	Goss	r-Goss	β /R	P	remainder
Cold rolled		5.9	1.2	13.4	4.8	50.9	4.3	19.8
316	1 min	6.0	1.2	13.5	5.1	49.2	4.2	20.8
	10 min	6.5	1.1	13.0	6.1	48.3	4.3	20.8
	20 min	6.8	1.2	12.3	5.4	47.9	4.3	22.1
	30 min	7.3	2.0	12.7	5.9	43.2	4.4	24.5
	40 min	7.7	2.8	11.8	6.1	40.4	4.4	26.8
	60 min	8.8	4.1	10.2	5.3	35.1	4.9	31.5
	80 min	9.6	5.2	9.0	6.2	30.3	4.9	34.7
	2 h	9.8	5.6	8.4	6.2	27.3	5.1	37.6
	5 h	9.1	5.9	8.2	7.0	25.4	5.3	39.1
343	1 min	6.0	1.0	13.3	5.3	51.3	4.8	18.2
	3 min	6.5	1.7	12.5	5.3	48.3	4.4	21.2
	4 min	6.5	1.9	12.7	6.0	46.3	4.6	22.0
	6 min	7.6	3.1	11.6	5.8	41.7	4.7	25.5
	7 min	7.9	4.3	11.2	6.2	35.0	5.2	30.2
	10 min	9.3	5.6	9.2	6.4	29.5	5.3	34.7
	15 min	10.0	6.0	8.2	6.5	26.2	5.3	37.8
	30 min	10.4	6.5	7.7	6.8	23.4	5.2	40.0
	1 h	10.3	6.5	8.2	6.9	23.2	5.0	40.0
371	2 s	6.2	1.2	12.9	6.3	48.1	4.5	20.8
	10 s	6.6	1.4	13.0	6.3	48.4	3.9	20.4
	20 s	7.0	1.8	12.1	5.6	46.7	4.1	22.7
	30 s	6.8	2.0	13.1	5.0	44.9	4.1	24.1
	40 s	8.3	3.6	10.4	5.5	38.7	4.5	29.0
	60 s	9.4	3.9	11.0	6.4	34.6	3.5	31.2
	80 s	9.7	5.9	8.5	6.9	27.4	4.8	36.9
	2 min	10.6	6.3	8.3	6.7	23.9	4.8	39.5
	5 min	10.4	6.6	8.0	7.2	22.9	5.3	39.6
	15 min	10.2	7.3	7.4	6.3	22.7	5.0	41.1
399	2 s	6.4	1.1	12.2	4.8	50.1	4.3	21.1
	5 s	6.4	1.2	12.6	5.5	49.7	4.3	20.2
	8 s	6.2	1.6	13.4	6.1	46.6	4.2	21.8
	10 s	7.3	2.0	12.6	5.3	44.2	4.7	23.9
	15 s	7.9	3.7	10.9	5.9	37.7	4.6	29.3
	20 s	9.5	5.3	8.8	6.1	30.5	5.0	34.8
	30 s	9.7	6.7	8.0	6.4	24.1	4.9	40.2
	1 min	9.9	6.9	7.5	7.0	22.0	4.9	41.8
427	2 s	6.6	1.7	13.0	6.1	45.8	4.1	22.7
	5 s	9.1	5.1	10.1	6.1	31.8	4.2	33.6
	10 s	10.0	6.7	7.8	7.5	21.3	4.8	43.9
	1 min	10.0	6.9	7.6	6.6	22.0	4.8	42.1
454	2 s	9.7	6.4	8.1	6.1	23.5	5.0	41.2
	10 s	10.2	7.5	7.5	6.6	20.9	4.8	42.5
482	2 s	9.4	7.8	7.7	7.3	20.2	4.9	42.6
	10 s	10.6	7.7	7.4	7.1	19.8	5.1	42.3

Table 8. Texture volume fractions for CC AA 3105 hot band annealed at 482°C for 6 h (D condition), cold rolled to 75% reduction, and then annealed at different temperatures for different times.

Temperature (°C)	Time	Texture volume fraction (%)						
		cube	r-cube	Goss	r-Goss	β /R	P	remainder
Cold rolled		7.2	1.5	12.7	5.1	49.5	4.1	19.9
343	10 s	7.1	1.1	14.0	5.8	47.2	4.4	20.5
	1 min	8.3	1.6	12.2	5.0	47.2	4.0	21.0
	5 min	8.1	1.7	12.4	4.9	47.1	4.0	21.8
	30 min	8.3	2.8	12.1	5.1	43.8	4.3	23.6
	1 h	8.2	2.7	11.9	6.1	43.6	4.6	22.9
	5 h	9.3	3.8	11.3	5.2	39.4	4.7	26.3
	12 h	9.5	3.9	11.1	5.6	39.5	5.4	25.0
	2 days	10.3	4.3	9.8	5.7	34.6	5.9	29.4
371	2 s	7.3	1.3	13.4	5.2	49.2	4.0	19.6
	10 s	7.7	1.4	12.8	5.2	48.9	4.2	19.7
	20 s	7.7	2.1	12.6	5.8	45.1	4.0	22.6
	60 s	8.8	3.3	11.3	6.2	40.4	4.4	25.6
	2 min	8.7	3.8	11.1	5.6	39.2	5.1	26.5
	5 min	8.9	4.4	10.7	6.4	35.3	5.6	28.7
	15 min	8.6	5.1	10.2	6.1	34.1	5.3	30.6
	1 h	9.3	5.1	9.2	6.1	32.0	5.9	32.3
	2 h	8.9	5.3	9.1	5.5	32.7	5.9	32.6
	5 h	9.0	6.0	9.3	6.3	31.1	5.8	32.5
399	2 s	8.2	1.4	12.3	5.1	48.2	3.8	21.1
	5 s	7.5	2.0	12.5	6.6	43.3	3.9	24.2
	8 s	8.2	3.4	11.5	5.7	40.0	4.4	26.8
	10 s	9.0	4.7	9.8	6.6	33.8	5.4	30.7
	20 s	8.5	5.7	9.2	6.5	31.5	5.6	33.0
	30 s	8.9	6.2	8.2	6.3	29.8	5.2	35.5
	1 min	8.4	6.6	8.6	6.0	29.9	6.0	34.6
427	2 s	7.5	2.1	12.3	5.4	45.2	4.5	23.0
	5 s	9.4	6.7	8.2	6.9	25.4	6.0	37.4
	10 s	9.3	7.4	7.4	7.3	21.8	5.9	40.8
	1 min	9.1	7.3	7.4	7.5	22.0	6.4	40.3
454	10 s	9.4	7.7	6.9	7.7	18.0	6.1	44.2
482	10 s	9.3	8.2	6.5	7.9	17.1	6.0	45.0

Table 9. Texture volume fractions for CC AA 3105 hot band annealed at 371°C for 6 h (F condition), cold rolled to 75% reduction, and then annealed at different temperatures for different times.

Temperature (°C)	Time	Texture volume fraction (%)						
		cube	r-cube	Goss	r-Goss	β /R	P	remainder
Cold rolled		5.7	0.3	9.8	3.1	66.5	4.1	10.5
316	1 min	5.4	0.4	10.0	2.8	66.7	4.6	10.1
	30 min	6.1	0.6	8.9	2.6	63.9	3.4	14.5
	2 days	5.4	1.4	9.2	3.8	61.4	6.7	12.1
343	10 s	5.1	0	10.4	3.7	67.0	4.1	9.7
	20 s	6.0	0.2	9.7	3.3	66.2	3.7	11.0
	1 min	6.2	1.0	9.6	3.7	62.2	4.5	12.8
	2 min	6.2	1.0	9.4	3.4	62.1	4.8	13.1
	5 min	6.7	2.2	8.9	3.8	53.5	7.0	17.9
	10 min	6.6	2.6	8.8	3.4	49.7	8.3	20.6
	30 min	7.2	3.6	8.4	3.7	44.5	8.6	24.0
	2 h	7.1	3.9	7.3	3.6	38.5	11.2	28.5
	5 h	6.4	4.9	7.7	3.7	38.2	11.5	27.6
371	2 s	6.0	0.2	10.3	3.1	64.9	4.1	11.4
	10 s	6.4	0.8	9.3	4.3	62.2	3.8	13.2
	15 s	6.4	1.6	9.4	4.2	54.6	5.3	18.5
	20 s	6.4	2.0	9.1	4.1	54.4	5.1	18.9
	30 s	7.1	2.6	9.4	4.5	47.7	6.5	22.2
	1 min	6.8	4.1	8.0	3.9	39.9	7.6	29.7
	2 min	6.3	4.6	8.0	4.6	37.4	7.6	31.5
	5 min	7.5	4.8	7.7	4.2	33.0	8.7	34.1
	15 min	6.5	5.5	8.1	4.4	32.0	9.4	34.1
399	2 s	6.4	0.4	9.9	3.8	63.7	4.2	11.6
	5 s	5.8	1.0	9.1	2.1	63.9	4.4	13.7
	8 s	6.4	2.5	8.9	3.8	52.1	5.6	20.7
	10 s	6.4	3.0	9.1	4.4	46.5	6.6	24.0
	15 s	7.0	5.2	8.3	4.6	31.0	8.2	35.7
	20 s	7.1	5.7	8.1	4.7	28.9	8.5	37.1
	1 min	6.2	6.4	7.9	4.8	25.1	8.5	41.1
	30 min	6.5	6.7	7.4	5.2	22.9	8.5	42.9
427	2 s	5.6	3.8	8.9	4.0	45.7	6.5	25.5
	5 s	6.6	6.5	8.3	5.2	24.9	7.8	40.7
	10 s	7.0	7.0	7.4	4.7	22.8	7.5	43.6
	1 min	6.5	7.2	7.9	5.5	20.6	8.7	43.6
454	10 s	6.3	7.6	7.7	5.7	19.0	7.6	46.1
482	10 s	6.5	7.8	7.7	5.9	17.9	8.1	46.1

Table 10. Texture volume fractions for CC AA 3105 hot band annealed at 599°C for 6 h and at 371°C for 6 h (G condition), cold rolled to 75% reduction, and then annealed at different temperatures for different times.

Temperature (°C)	Time	Texture volume fraction (%)						
		cube	r-cube	Goss	r-Goss	β /R	P	remainder
Cold rolled		6.3	1.7	12.2	6.0	48.0	4.8	21.3
316	1 min	6.3	2.3	11.5	5.5	47.7	4.0	22.7
	3 min	6.6	1.9	11.4	5.9	47.7	4.4	22.1
	8 min	6.7	2.3	10.4	5.8	46.3	5.1	23.5
	10 min	8.9	3.0	10.5	6.7	41.7	4.0	25.3
	12 min	8.7	3.3	10.5	5.8	40.8	4.6	26.3
	15 min	9.9	3.7	10.2	5.6	37.9	4.3	28.4
	20 min	11.2	4.9	10.1	6.1	35.2	4.2	28.3
	30 min	12.0	5.3	9.3	6.3	30.8	4.6	31.6
	1 h	12.7	6.0	7.9	6.1	26.2	5.1	36.0
	2 h	13.1	6.5	7.9	6.8	25.8	4.7	35.2
343	2 s	5.6	1.1	12.3	5.7	51.0	4.2	20.1
	10 s	6.6	1.9	11.0	6.3	48.3	4.7	21.2
	40 s	7.2	2.3	11.5	5.8	47.0	3.7	22.5
	60 s	8.6	2.6	10.9	5.5	45.0	4.2	23.2
	90 s	10.8	3.8	10.2	6.4	36.3	4.2	28.3
	2 min	11.0	4.6	9.7	6.2	35.2	3.9	29.4
	3 min	12.1	6.1	8.3	6.0	27.3	5.0	35.2
	5 min	13.0	7.0	7.2	6.9	22.6	5.2	38.1
	10 min	12.7	7.2	7.8	6.6	22.5	5.0	38.2
371	2 s	7.1	1.6	11.1	6.0	48.3	4.0	21.9
	10 s	7.5	1.8	11.2	5.7	47.3	4.1	22.4
	15 s	9.5	3.4	9.7	6.4	39.9	4.5	26.6
	20 s	10.0	4.3	10.4	6.7	37.5	4.0	27.2
	25 s	11.2	5.8	8.5	7.0	28.0	4.8	34.7
	30 s	12.3	6.2	8.0	7.0	25.2	5.1	36.2
	1 min	12.6	7.2	7.5	6.7	21.0	4.8	40.2
	2 min	12.5	7.0	7.7	7.2	21.0	4.9	39.7
399	2 s	6.6	1.4	10.8	5.4	50.0	4.6	21.2
	5 s	6.3	2.2	11.2	5.0	47.2	4.8	23.3
	8 s	9.8	4.6	9.6	6.0	35.0	4.7	30.2
	10 s	10.2	5.0	9.4	6.2	34.4	5.0	29.8
	15 s	12.0	7.6	7.5	7.2	20.7	5.3	39.7
	20 s	12.5	8.1	7.1	7.8	19.6	5.3	39.6
	1 min	11.8	7.9	7.2	7.8	19.4	5.2	40.7
427	10 s	12.0	7.7	6.9	7.3	18.7	4.8	42.6
	1 min	12.3	7.7	7.1	7.6	18.4	5.1	41.8
454	10 s	12.2	8.0	7.0	7.8	18.8	5.1	41.1
482	10 s	13.1	8.0	6.5	7.7	17.5	5.1	42.1

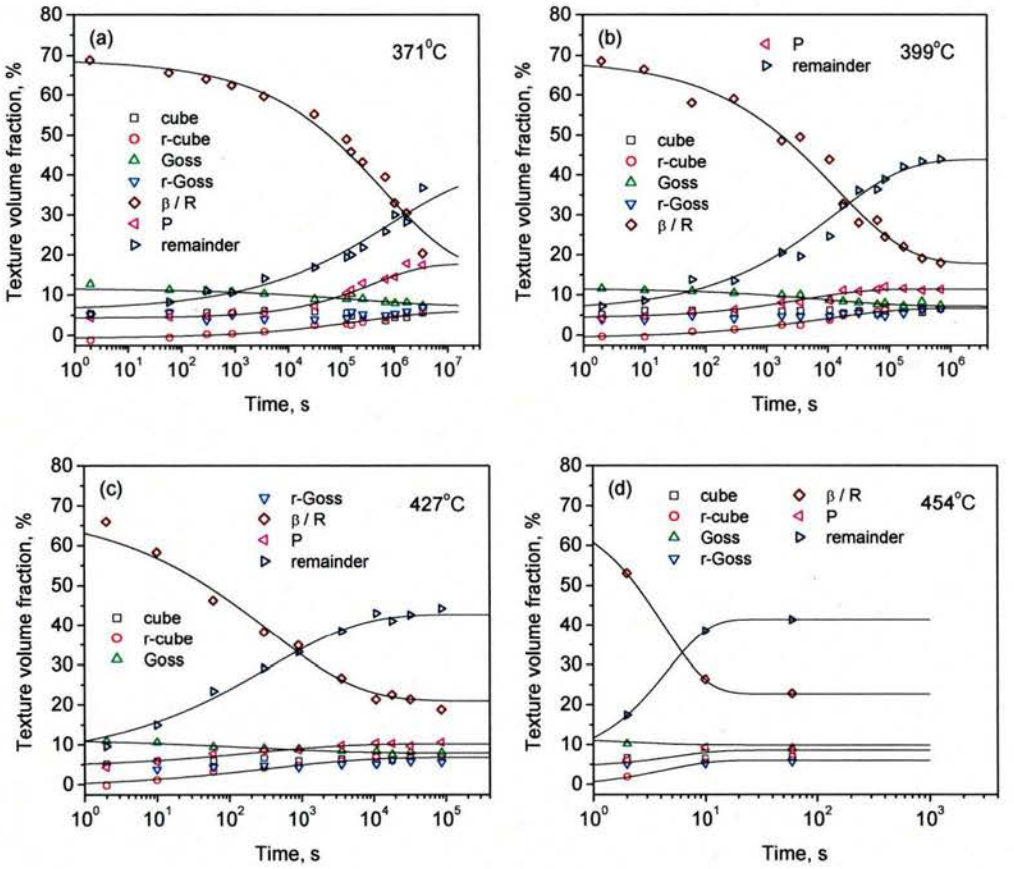

Fig. 30. Plots of texture volume fractions as a function of annealing time at temperatures of (a) 371, (b) 399, (c) 427, and (d) 454°C for CC AA 3105 aluminum alloy under the A condition.

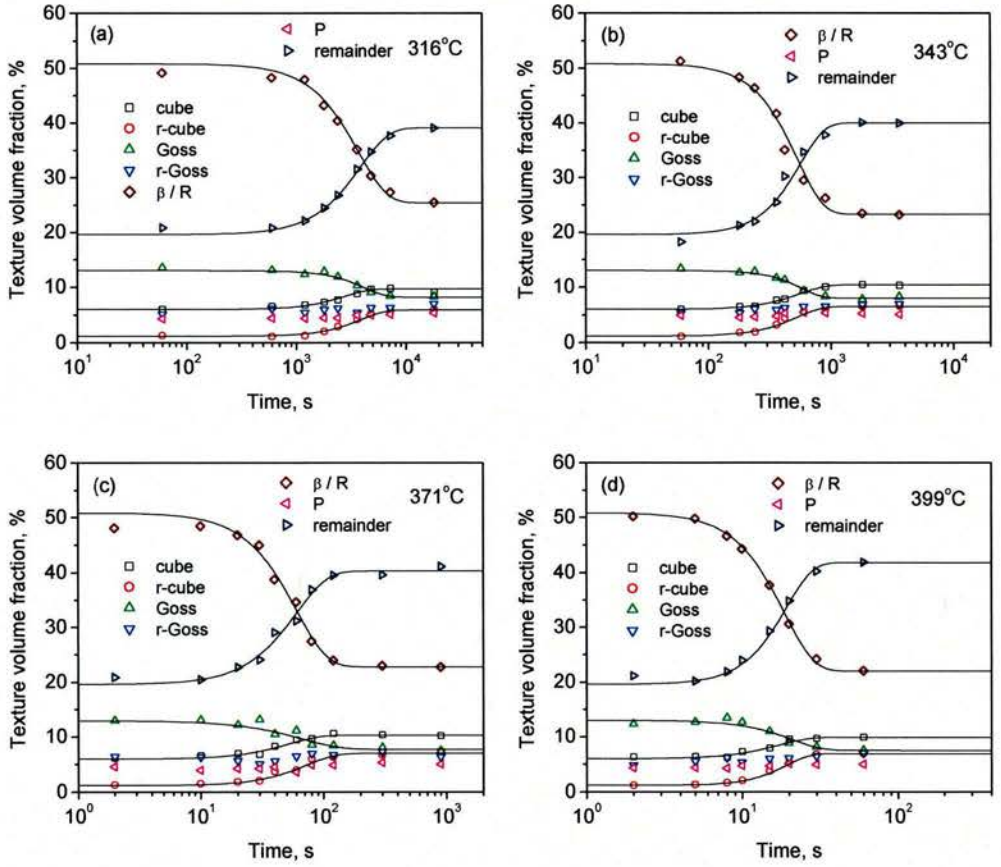

Fig. 31. Plots of texture volume fractions as a function of annealing time at temperatures of (a) 316, (b) 343, (c) 371, and (d) 399°C for CC AA 3105 aluminum alloy under the B condition.

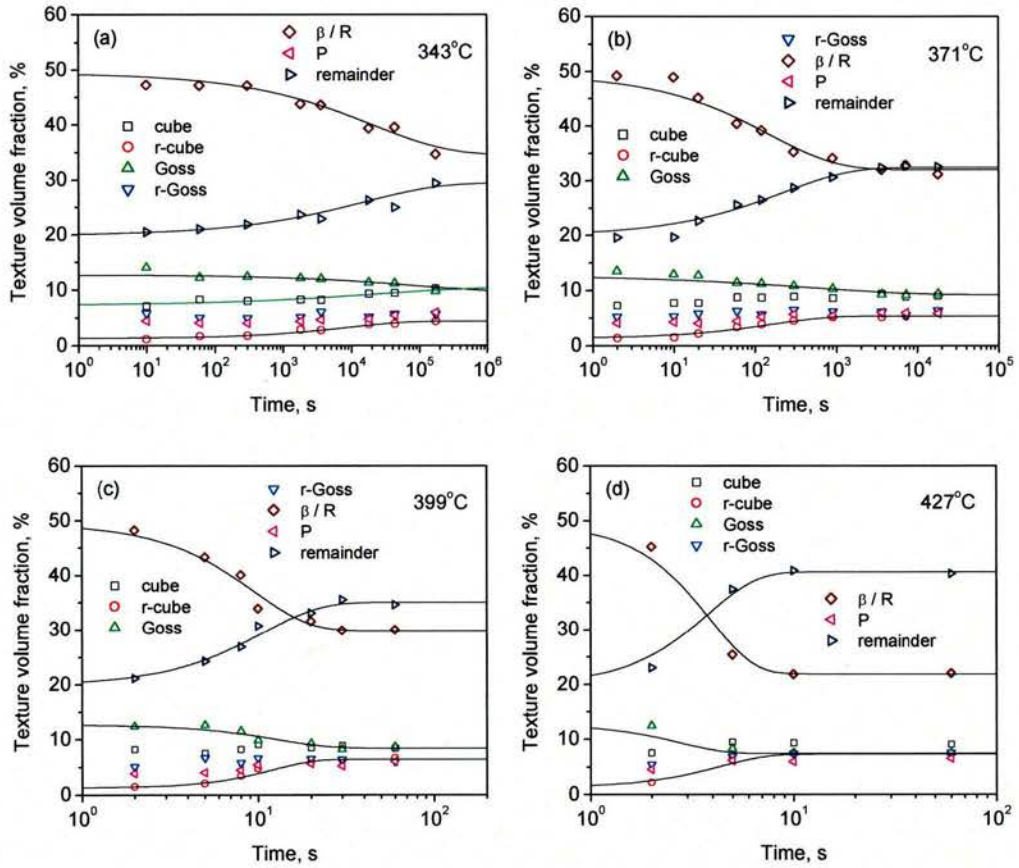

Fig. 32. Plots of texture volume fractions as a function of annealing time at temperatures of (a) 343, (b) 371, (c) 399, and (d) 427°C for CC AA 3105 aluminum alloy under the D condition.

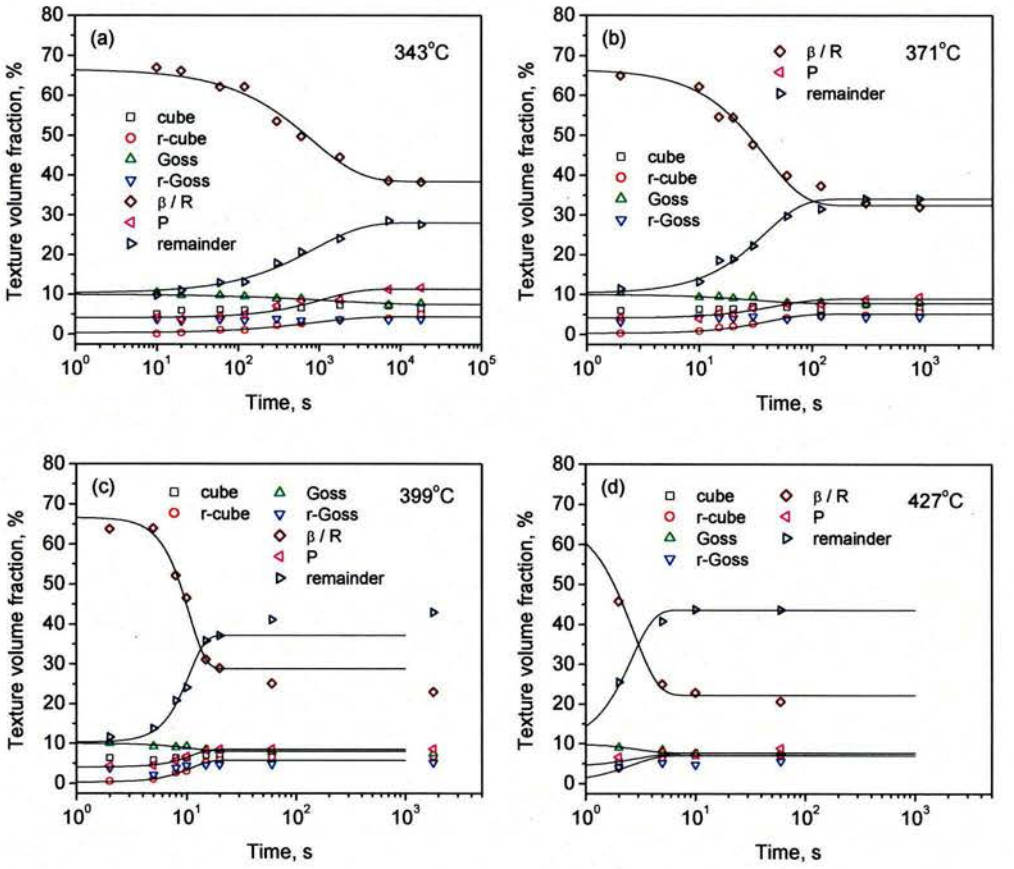

Fig. 33. Plots of texture volume fractions as a function of annealing time at temperatures of (a) 343, (b) 371, (c) 399, and (d) 427°C for CC AA 3105 aluminum alloy under the F condition.

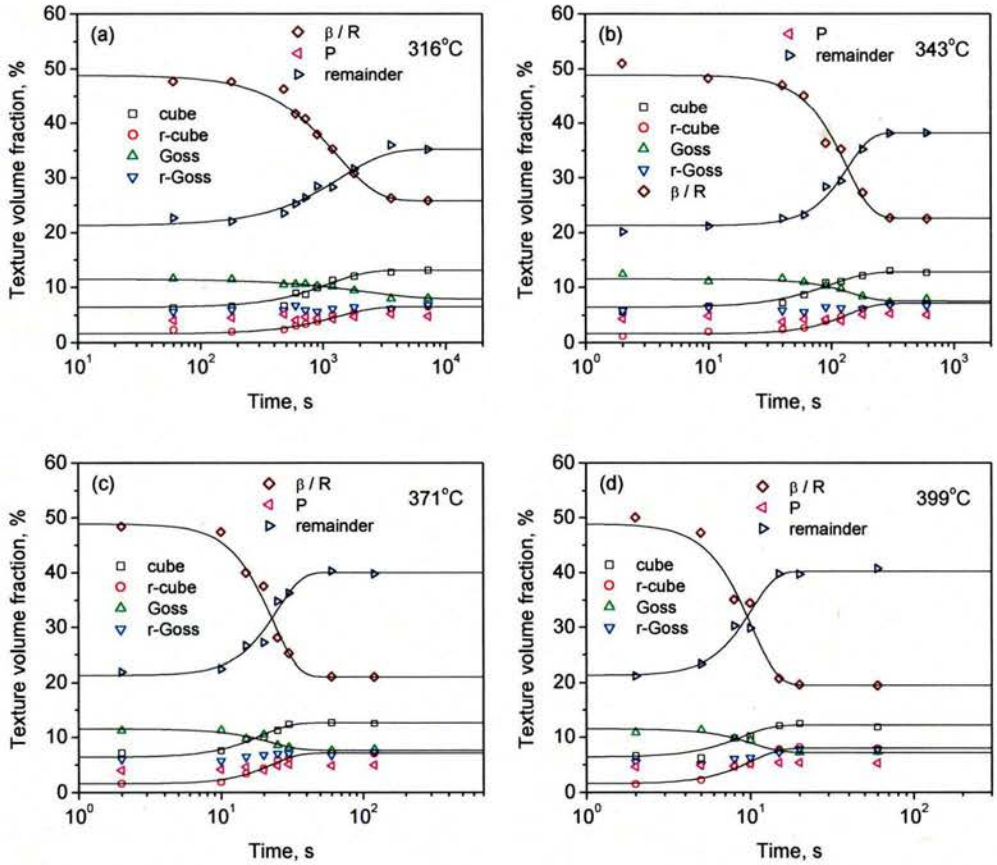

Fig. 34. Plots of texture volume fractions as a function of annealing time at temperatures of (a) 316, (b) 343, (c) 371, and (d) 399°C for CC AA 3105 aluminum alloy under the G condition.

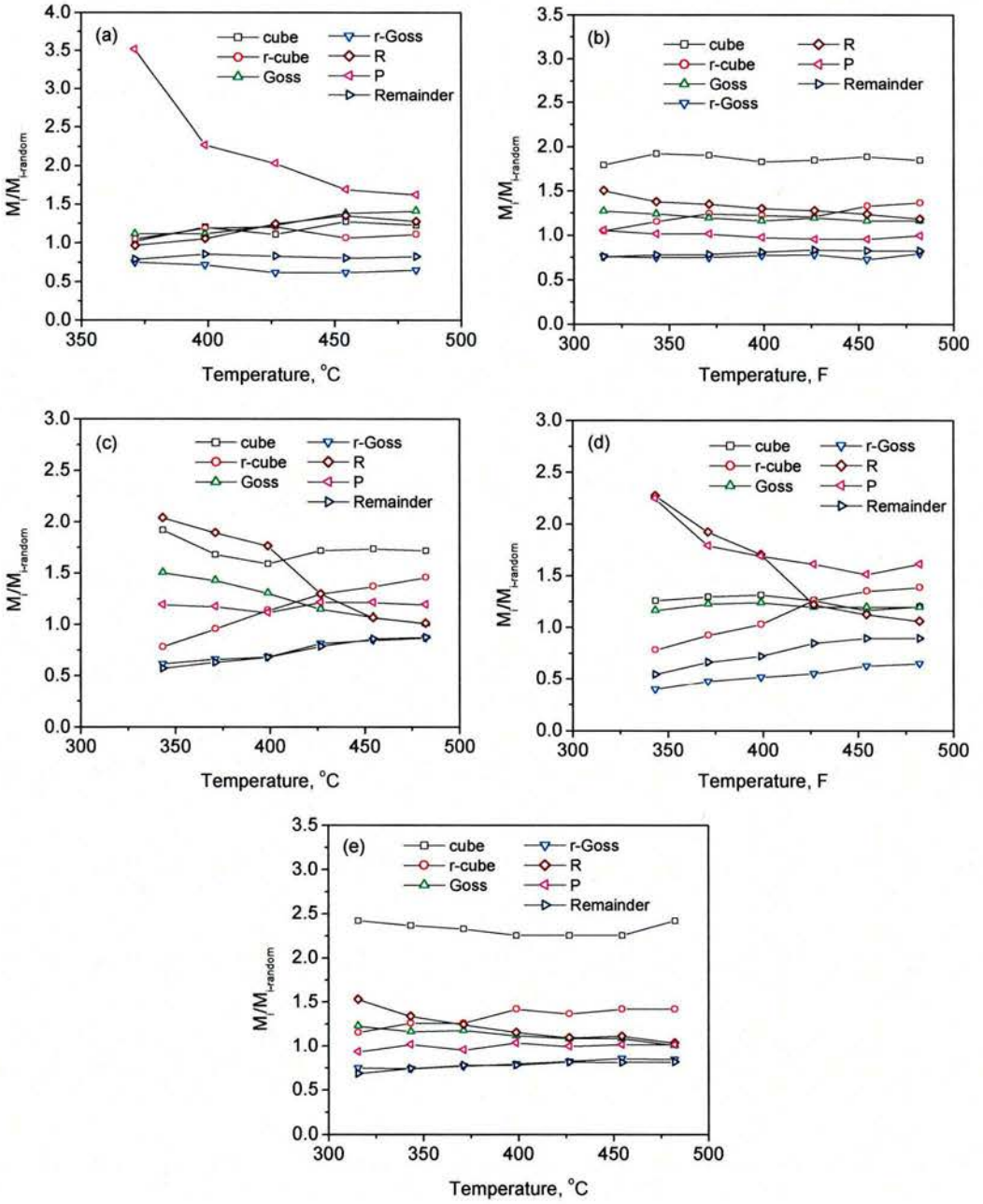

Fig. 35. Effect of annealing temperature on the recrystallization texture of CC AA 3105 aluminum alloy. (a) No pre-treatment, (b) 599°C for 6 h, (c) 482°C for 6 h, (d) 371°C for 6 h, and (e) 599°C for 6 h + 371°C for 6 h. M_i represents the volume fraction of different texture components, and $M_{i\text{-}random}$ represents the volume fraction of the texture component under a random condition.

annealing temperature. At low temperatures the recrystallization texture consisted of strong P and R components. As the annealing temperature increased, the strengths of the P and R components decreased, whereas the strengths of the r-cube, r-Goss and remainder components increased. At high temperatures the recrystallization texture consisted of a weak P component.

For the CC AA 3105 aluminum alloy under the G condition, the recrystallization texture consisted of a strong cube component. As the annealing temperature increased, the strength of the R component decreased slightly, whereas the strength of the r-cube component increased slightly. The strengths of the other components hardly varied with the annealing temperature. The change in the texture components during recrystallization was similar to that under the B condition.

The variation in texture volume fractions during isothermal annealing can be defined by

$$f(t) = \frac{M(t) - M(0)}{M(\infty) - M(0)} \tag{6}$$

where $M(0)$, $M(t)$ and $M(\infty)$ are the texture volume fractions corresponding to a texture component at the beginning, at time t and at the end of the recrystallization process, respectively. According to the work of Hansen *et al.* [29] and Liu *et al.* [30], the relationship between $f(t)$ and annealing time can be also described by the JMAK equation. The values of k and n, which were determined by fitting the experimental data into Equation (4), and the values of $M(0)$ and $M(\infty)$ are listed in Tables 11 to 15 for CC AA 3105 aluminum alloy with different pre-treatments, respectively. Note that the values of k and n for some components in CC AA 3105 aluminum alloy with different pre-treatments were not obtained due to a slight change in these components. It is seen from Tables 11 and 15 that the n value depended strongly on the pre-treatment prior to cold rolling. Under the A condition, the n value was estimated to be about 0.35. The low n value should reflect the effect of Zener-particle pinning caused by concurrent precipitation on recrystallization texture, as discussed latter. Under the B condition, the n value of around 2.0 was consistent with other results on aluminum alloys [31,32], although this value is smaller than that expected from classical analysis. Under the D condition, at 343°C the n value was estimated to be about 0.4. As the annealing temperature increased to 399°C, the n value increased to 1.4. Under the F condition, the n value ranged between 0.8 and 2.8, and it increased with increasing annealing temperature. Under the G condition, the n value ranged between 1.3 and 2.8, and it increased with increasing annealing temperature. The parameters $M(0)$, $M(\infty)$, k and n describe the formation or disappearance of a given texture component during isothermal annealing. Therefore, the evolution of recrystallization texture in CC AA 3105 aluminum alloy can be predicted from the values of $M(0)$, $M(\infty)$, k and n.

The activation energy for recrystallization of CC AA 3105 aluminum alloy with different pre-treatments has been estimated from measurements of hardness, as mentioned in Section 3.1.3. However, the activation energy for recrystallization of the alloy without pre-treatment (A condition) can not be determined by the same method. On the other hand, the recrystallization progress can be revealed by texture evolution. Thus, the time to 50% recrystallization ($t_{0.5}$) can be derived from texture data, as shown in Fig. 18. Since the $t_{0.5}$ value is almost the same for different texture components, only a value from the β/R component is shown in Fig. 18. It is noted from Fig. 18 that the Q_{RX} value estimated from texture data is in reasonable agreement with that from measurements of hardness. The activation energy for recrystallization of CC AA 3105 aluminum alloy without pre-treatment was determined from texture data to be 508 kJ/mole, which is obviously higher than that for the alloy under the other conditions.

Table 11. Values of $M(0)$, $M(\infty)$, k and n for different components of cold rolled AA 3105 aluminum alloy under the A condition during isothermal annealing at different temperatures.

Temperature, (°C)	Component	$M(0)$, %	$M(\infty)$, %	k	n
371	cube	5.0	5.5	---	---
	r-cube	-0.7	5.9	$1.7 \cdot 10^{-2}$	0.33
	Goss	11.6	7.2	$4.0 \cdot 10^{-2}$	0.26
	r-Goss	4.5	6.8	---	---
	β fiber / R	69.0	16.3	$1.2 \cdot 10^{-2}$	0.33
	P	4.3	17.7	$2.7 \cdot 10^{-3}$	0.46
	remainder	6.2	40.5	$1.9 \cdot 10^{-2}$	0.29
399	cube	5.0	6.5	---	---
	r-cube	-0.7	6.7	$4.4 \cdot 10^{-2}$	0.34
	Goss	11.6	7.2	$4.7 \cdot 10^{-2}$	0.34
	r-Goss	4.5	6.5	---	---
	β fiber / R	69.0	17.8	$2.9 \cdot 10^{-2}$	0.37
	P	4.3	11.4	$3.1 \cdot 10^{-2}$	0.42
	remainder	6.2	43.9	$3.0 \cdot 10^{-2}$	0.37
427	cube	5.0	6.0	---	
	r-cube	-0.7	6.8	$1.5 \cdot 10^{-1}$	0.32
	Goss	11.6	7.9	$2.3 \cdot 10^{-1}$	0.28
	r-Goss	4.5	5.6	---	---
	β fiber / R	69.0	21.0	$1.3 \cdot 10^{-1}$	0.34
	P	4.3	10.2	$1.6 \cdot 10^{-1}$	0.33
	remainder	6.2	42.7	$1.4 \cdot 10^{-1}$	0.34

Table 12. Values of $M(0)$, $M(\infty)$, k and n for different components of cold rolled AA 3105 aluminum alloy under the B condition during isothermal annealing at different temperatures.

Temperature, (°C)	Component	$M(0)$, %	$M(\infty)$, %	k	n
316	cube	6.0	9.7	$3.1 \cdot 10^{-7}$	1.9
	r-cube	1.2	5.9	$7.1 \cdot 10^{-8}$	2.0
	Goss	13.0	8.2	$2.0 \cdot 10^{-8}$	2.1
	r-Goss	5.0	6.9	---	---
	β fiber / R	50.9	25.4	$1.2 \cdot 10^{-6}$	1.7
	P	4.3	5.3	---	---
	remainder	19.6	39.1	$1.1 \cdot 10^{-6}$	1.7
343	cube	6.0	10.4	$2.1 \cdot 10^{-6}$	2.1
	r-cube	1.2	6.5	$1.4 \cdot 10^{-6}$	2.2
	Goss	13.0	8.0	$1.2 \cdot 10^{-7}$	2.5
	r-Goss	5.0	6.8	---	---
	β fiber / R	50.9	23.3	$2.7 \cdot 10^{-6}$	2.0
	P	4.3	5.1	---	---
	remainder	19.6	40.0	$9.3 \cdot 10^{-7}$	2.2
371	cube	6.0	10.3	$1.1 \cdot 10^{-3}$	1.7
	r-cube	1.2	7.0	$4.4 \cdot 10^{-4}$	1.8
	Goss	13.0	7.7	$3.4 \cdot 10^{-3}$	1.4
	r-Goss	5.0	6.8	---	---
	β fiber / R	50.9	22.8	$7.7 \cdot 10^{-4}$	1.7
	P	4.3	5.1	---	---
	remainder	19.6	40.3	$8.6 \cdot 10^{-4}$	1.7
399	cube	6.0	9.9	$2.0 \cdot 10^{-3}$	2.2
	r-cube	1.2	6.9	$1.9 \cdot 10^{-5}$	2.9
	Goss	13.0	7.5	$1.2 \cdot 10^{-3}$	2.2
	r-Goss	5.0	7.0	---	---
	β fiber / R	50.9	22.0	$1.2 \cdot 10^{-3}$	2.3
	P	4.3	4.9	---	---
	remainder	19.6	41.8	$4.6 \cdot 10^{-4}$	2.6

Table 13. Values of $M(0)$, $M(\infty)$, k and n for different components of cold rolled AA 3105 aluminum alloy under the D condition during isothermal annealing at different temperatures.

Temperature, (°C)	Component	$M(0)$, %	$M(\infty)$, %	k	n
343	cube	7.2	10.4	$4.4 \cdot 10^{-2}$	0.31
	r-cube	1.3	4.4	$1.0 \cdot 10^{-2}$	0.51
	Goss	12.7	9.7	$1.4 \cdot 10^{-2}$	0.38
	r-Goss	5.2	5.6	---	---
	β fiber / R	49.5	34.5	$2.2 \cdot 10^{-2}$	0.38
	P	4.1	6.0	---	---
	remainder	19.9	24.9	$2.3 \cdot 10^{-2}$	0.39
371	cube	7.2	9.1	---	---
	r-cube	1.3	5.4	$4.4 \cdot 10^{-2}$	0.61
	Goss	12.7	9.2	$1.2 \cdot 10^{-1}$	0.34
	r-Goss	5.2	6.0	---	---
	β fiber / R	49.5	32.0	$7.1 \cdot 10^{-2}$	0.52
	P	4.1	5.9	---	---
	remainder	19.9	32.4	$6.0 \cdot 10^{-2}$	0.52
399	cube	7.2	8.6	---	---
	r-cube	1.3	6.4	$9.3 \cdot 10^{-2}$	1.8
	Goss	12.7	8.4	$2.3 \cdot 10^{-2}$	1.5
	r-Goss	5.2	6.2	---	---
	β fiber / R	49.5	29.8	$4.5 \cdot 10^{-2}$	1.4
	P	4.1	5.6	---	---
	remainder	19.9	35.0	$4.4 \cdot 10^{-2}$	1.3

Table 14. Values of $M(0)$, $M(\infty)$, k and n for different components of cold rolled AA 3105 aluminum alloy under the F condition during isothermal annealing at different temperatures.

Temperature, (°C)	Component	$M(0)$, %	$M(\infty)$, %	k	n
343	cube	5.4	6.8	---	---
	r-cube	0.3	4.4	$9.4 \cdot 10^{-3}$	0.69
	Goss	10.0	7.5	$2.0 \cdot 10^{-2}$	0.54
	r-Goss	3.3	3.6	---	---
	β fiber / R	66.6	38.4	$8.0 \cdot 10^{-3}$	0.72
	P	4.1	11.3	$1.5 \cdot 10^{-3}$	0.93
	remainder	10.3	28.0	$7.2 \cdot 10^{-3}$	0.73
371	cube	5.4	7.0	---	---
	r-cube	0.3	5.2	$5.7 \cdot 10^{-3}$	1.38
	Goss	10.0	7.9	$1.6 \cdot 10^{-2}$	1.19
	r-Goss	3.3	4.3	---	---
	β fiber / R	66.6	32.5	$1.0 \cdot 10^{-2}$	1.25
	P	4.1	9.0	$7.8 \cdot 10^{-3}$	1.25
	remainder	10.3	34.1	$8.6 \cdot 10^{-3}$	1.31
399	cube	5.4	7.1	---	---
	r-cube	0.3	5.8	$3.3 \cdot 10^{-3}$	2.40
	Goss	10.0	8.0	$1.1 \cdot 10^{-2}$	1.90
	r-Goss	3.3	4.7	---	---
	β fiber / R	66.6	28.8	$1.1 \cdot 10^{-3}$	2.88
	P	4.1	8.5	$1.6 \cdot 10^{-3}$	2.70
	remainder	10.3	37.1	$9.5 \cdot 10^{-4}$	2.95

Table 15. Values of $M(0)$, $M(\infty)$, k and n for different components of cold rolled AA 3105 aluminum alloy under the G condition during isothermal annealing at different temperatures.

Temperature, (°C)	Component	$M(0)$, %	$M(\infty)$, %	k	n
316	cube	6.4	13.1	$5.3 \cdot 10^{-5}$	1.4
	r-cube	1.6	6.5	$4.2 \cdot 10^{-5}$	1.4
	Goss	11.5	7.9	$6.8 \cdot 10^{-4}$	1.0
	r-Goss	5.9	6.8	---	---
	β fiber / R	48.9	25.8	$8.6 \cdot 10^{-5}$	1.3
	P	4.4	4.7	---	---
	remainder	21.3	35.2	$1.9 \cdot 10^{-4}$	1.2
343	cube	6.4	12.8	$1.5 \cdot 10^{-3}$	1.4
	r-cube	1.6	7.1	$8.3 \cdot 10^{-5}$	1.9
	Goss	11.5	7.5	$5.5 \cdot 10^{-5}$	2.0
	r-Goss	5.9	6.7	---	---
	β fiber / R	48.9	22.6	$4.1 \cdot 10^{-5}$	2.1
	P	4.4	5.1	---	---
	remainder	21.3	38.2	$1.1 \cdot 10^{-5}$	2.3
371	cube	6.4	12.6	$2.1 \cdot 10^{-3}$	2.1
	r-cube	1.6	7.1	$6.4 \cdot 10^{-4}$	2.4
	Goss	11.5	7.6	$1.3 \cdot 10^{-3}$	2.1
	r-Goss	5.9	7.0	---	---
	β fiber / R	48.9	21.0	$4.5 \cdot 10^{-4}$	2.4
	P	4.4	4.8	---	---
	remainder	21.3	40.0	$2.9 \cdot 10^{-4}$	2.5
399	cube	6.4	12.2	$5.8 \cdot 10^{-3}$	2.4
	r-cube	1.6	8.0	$3.0 \cdot 10^{-3}$	2.5
	Goss	11.5	7.2	$2.1 \cdot 10^{-3}$	2.6
	r-Goss	5.9	7.8	---	---
	β fiber / R	48.9	19.5	$1.7 \cdot 10^{-3}$	2.7
	P	4.4	5.2	---	---
	remainder	21.3	40.2	$1.0 \cdot 10^{-4}$	2.9

4. Discussion

4.1. Kinetics of recrystallization

The recrystallization kinetics of CC AA 3105 aluminum alloy with different pre-treatments has been quantitatively analyzed by measurements of texture. Fig. 36 shows the comparison of the start (10%) and finish (90%) of recrystallization among these different pre-heat treatment conditions. It is noted that the pre-treatment prior to cold rolling strongly affects the recrystallization behavior of CC AA 3105 aluminum alloys. Under the A condition where the hot band was directly cold rolled to 75% reduction, the recrystallization progress is markedly retarded compared with the recrystallization under the B condition (Fig. 36(a)). This suggests that the pre-treatment at 599°C prior to cold rolling significantly stimulates the recrystallization of CC AA 3105 aluminum alloy. By comparing the TTT diagrams for recrystallization between the A and F conditions (Fig. 36 (b)), it is seen that the heat treatment of precipitation at 371°C also significantly stimulates recrystallization. In addition, the preheating temperature also affects the recrystallization behavior of CC AA 3105 aluminum alloy (Fig. 36(c)). The recrystallization progress under the D condition is slower than that under the B condition. At 343°C the time to reach complete recrystallization under the D condition is much longer than that under the B condition. Fig. 36(d) shows the effect of additional treatment on recrystallization. It is clear that the additional heat treatment at 371°C further stimulates the recrystallization of CC AA 3105 aluminum alloy.

The effect of the pre-treatment on recrystallization kinetics is related to the variation in microstructure prior to cold rolling. In CC processing, the continuous cast slabs possess an equiaxed grain structure and a random texture [33]. No recrystallization occurs during hot rolling. The CC hot band retains a large amount of elements in solid solution due to the rapid cooling rate of the CC slab and a relatively rapidly falling temperature during hot rolling. After the CC hot band is heat-treated at 599°C for 6 h, the deformed microstructure is fully recrystallized. At the same time, more particles precipitate from the supersaturated matrix, leading to a decrease in the amount of elements in solid solution. The constitutional change can be confirmed by measurements of the electrical resistivity. The electrical resistivity of the CC AA 3105 hot band was measured to be 4.62 μΩ·cm, which decreased to 4.16 μΩ·cm after pre-heating at 599°C.

The kinetics of recrystallization depends on the nucleation site density, the stored energy and the effect of precipitates on recrystallization. The directly cold rolled sample without pre-treatment has a higher nucleation site density than the cold rolled samples with pre-treatment [6]. The stored energy is related to the internal dislocation density, the misorientation and spacing of dislocation walls. The stored energy of the cold rolled samples without pre-treatment can be estimated to be larger than that of the cold rolled samples with a pre-treatment of 599°C due to the high total rolling reduction of the former. If the recrystallization behavior were considered only from the nucleation site density arising mainly from the grain boundaries and the stored energy, the alloy without pre-treatment would be easier to recrystallize. However, this inference is contrary to the experimental results shown in Fig. 36(a). It is clear that the precipitates in CC AA 3105 aluminum alloy have a strong effect on recrystallization kinetics.

The precipitates in aluminum alloys are either already present in the as-deformed state or formed during recrystallization annealing. In order to quantify the amount of precipitates formed during recrystallization annealing, the electrical resistivity of these cold rolled and annealed sheets was measured, and the results are shown in Fig. 37. It is seen that the electrical resistivity decreased drastically with increasing annealing time under the A condition. A large amount of

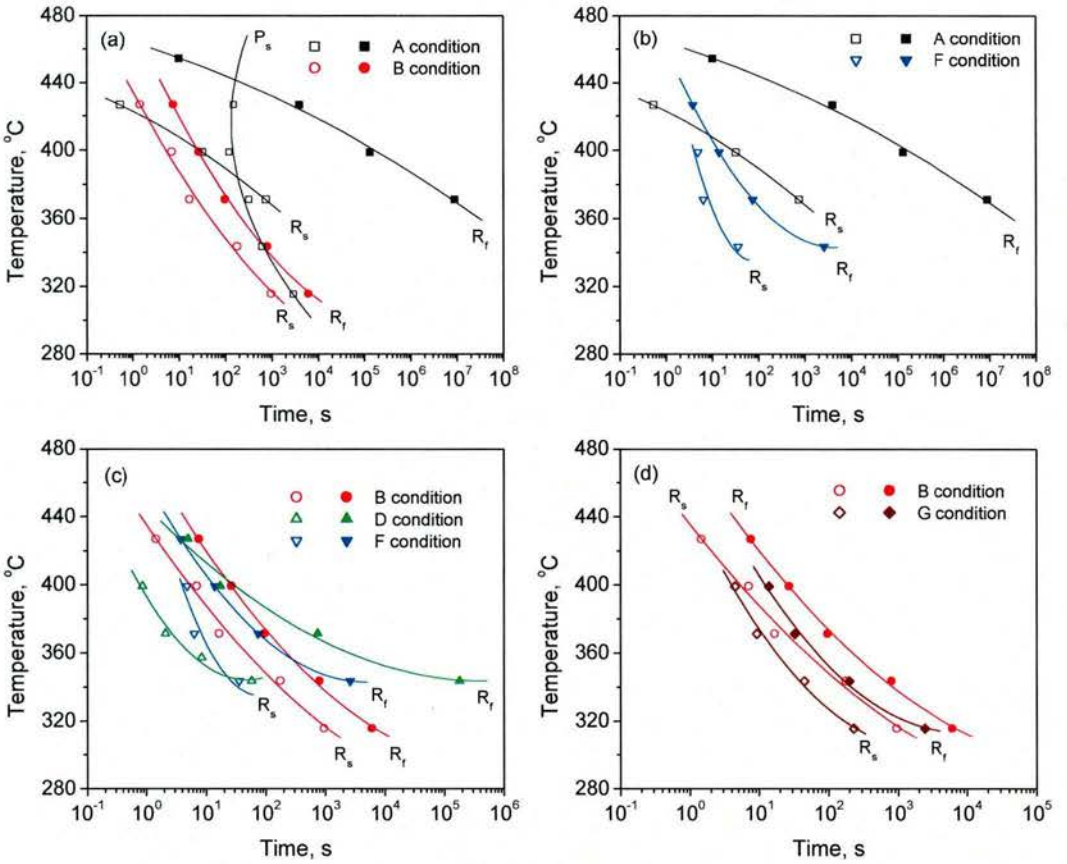

Fig. 36. Time-Temperature-Transformation (TTT) diagrams for the recrystallization and precipitation of CC AA 3105 aluminum alloy with different pre-treatments. R_S: the start (10%) of recrystallization; R_f: the finish (90%) of recrystallization; P_S: the start of precipitation defined by a decrease of 0.3 in electrical resistivity.

precipitation is expected to occur during annealing of the alloy without pre-treatment. If it is assumed that the amount of precipitation corresponding to the decrease of 0.3 in the electrical resistivity exerts an influence on recrystallization, then the Time-Temperature-Transformation (TTT) diagrams for precipitation can be plotted, as shown in Fig. 36(a). For CC AA 3105 aluminum alloy without pre-treatment, annealing at 427°C only results in a small amount of precipitation before the finish of recrystallization, indicating the slight effect on recrystallization. As the annealing temperature decreases, the amount of precipitation before the onset of recrystallization and during recrystallization increases, which strongly retards recrystallization.

Under the other conditions of B, D, F and G, more alloying elements are precipitated from the supersaturated matrix during the pre-treatments. In these cases the potential for concurrent precipitation during recrystallization annealing is considerably decreased. Thus, the amount of concurrent precipitation is weaker before complete recrystallization. This indicates that the progress of recrystallization is not affected by concurrent precipitation, but predominately by precipitates present in the as-deformed state.

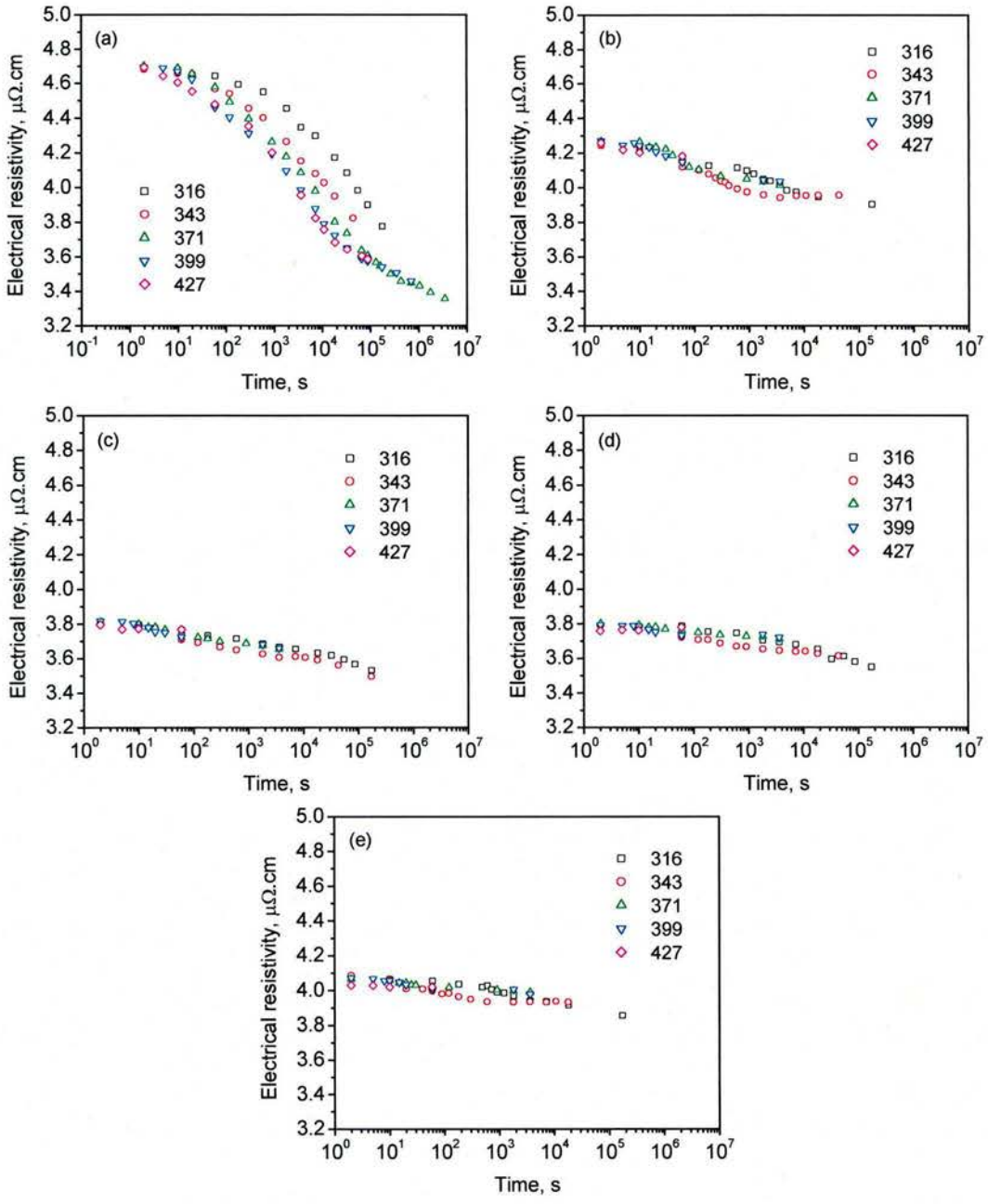

Fig. 37. Electrical resistivity of CC AA 3015 aluminum alloy with different pre-treatments as a function of annealing time at different temperatures. (a) No pre-treatment, (b) 599°C for 6 h, (c) 482°C for 6 h, (d) 371°C for 6 h, and (e) 599°C for 6 h + 371°C for 6 h.

The preheating temperature strongly affects the amount and size of precipitates present in the as-deformed state. As the preheating temperature decreases, the amount of precipitation increases, whereas the size of the precipitates decreases. Therefore, the large precipitates formed during the pre-heat treatment of 599°C for 6 h generally promote recrystallization by particle stimulated nucleation (PSN), whereas the fine precipitates formed during the preheat treatment of 482°C for 6 h retard recrystallization. The deformed microstructure is not recrystallized after the hot band is preheat treated at 371°C for 6 h. High nucleation site density and stored energy promote recrystallization. However, at the same time finely dispersed precipitates retard recrystallization. In the double treatment case (G condition), the deformed structure is fully recrystallized after preheating at 599°C. Thus, the size of the precipitates produced by the additional treatment of 371°C is relatively large. These relatively large precipitates promote recrystallization.

The progress of recrystallization is well described by the n value in the JMAK equation and the apparent activation energy for recrystallization. Based on the measurements of hardness and textures, the n value was estimated for CC AA 3105 aluminum alloy with different pre-treatments, as shown in Tables 5 and 11 to 15. The n value of around 2.0 in the alloy with a pre-treatment (B condition) is consistent with other results on aluminum alloys [31,32], although this value is smaller than that expected from the classical analysis. However, a very low value of n = 0.35 was found in CC AA 3105 aluminum alloy without pre-treatment (A condition). Such a difference in the n value between the alloy with and without pre-treatment may be attributed to the effect of concurrent precipitation on recrystallization. Daaland and Nes [1] have pointed out that a low n value in Al-Mn-Mg alloys is accounted for by the concurrent precipitation reaction. Concurrent precipitation retards the recrystallization process. In addition, under the D and F conditions the n value increases with increasing annealing temperature. The low n value at low temperatures is attributed to the effect of precipitates present in the as-deformed state.

It is known that the activation energy for recrystallization is strongly affected by solution of solutes and by precipitation. In the present work, the activation energy (Q) for recrystallization of CC AA 3105 aluminum alloy with a pre-treatment (B condition) was determined to be 214 kJ/mol. However, the activation energy for recrystallization of the alloy without pre-treatment was estimated to be 508 kJ/mole. It is clear that concurrent precipitation increases the activation energy for recrystallization. In addition, fine precipitates present in the as-deformed state also increase the activation energy for recrystallization, as shown in Fig. 18 for the pre-treatments of 482°C and 371°C.

4.2. Recrystallized grains

The observation of recrystallized grains reveals that CC AA 3105 aluminum alloy without pre-treatment exhibits a microstructure transition from a coarse elongated grain structure to a fine equiaxed grain structure with increasing annealing temperature. A similar transition has been observed in cold rolled supersaturated Al-Mn-Mg [1] and Al-Mn [3] alloys. The coarse elongated grain structure in 3xxx series aluminum alloys usually accompanies the P and ND rotated cube textures. Daaland and Nes [1] studied the evolution of grain sizes with different orientations during annealing in Al-Mn-Mg alloys. They found that the P and ND rotated cube oriented grains grew significantly faster than the random component. A recent investigation on an Al-1.3 wt-%Mn by Somerday and Humphreys [5] demonstrated that recrystallized grains were elongated due to Zener pinning arising from precipitation on the prior high angle grain boundaries. Since the high angle grain boundaries are aligned in the RD, the precipitates inhibit growth in the ND. Therefore, the coarse elongated grain structure can be attributed to the Zener pinning effect.

Thus, the microstructure transition observed in the present work can be explained based on the effect of concurrent precipitation. During low temperature annealing of CC AA 3105 aluminum alloy without pre-treatment, precipitation occurs preferentially at high angle grain boundaries before the onset of recrystallization. Due to the Zener pinning effect, coarse elongated grains are observed. As the annealing temperature increases, recrystallization occurs more rapidly than precipitation, creating less interaction of the two processes. The size of recrystallized grains is reduced. At high temperatures recrystallization is finished before substantial precipitation occurs, and a fine grain structure is obtained. After CC AA 3105 aluminum alloy is pre-heat treated at 599°C for 6 hours, the solute supersaturation is decreased as a result of precipitation of large particles from the supersaturated matrix. The resulting low solute supersaturation provides little driving force for heterogeneous precipitation. Therefore, the size of recrystallized grain under the B condition is very small.

4.3. Recrystallization texture

The preheat treatment strongly affects not only the recrystallization of CC AA 3105 aluminum alloy, but also the evolution of recrystallization texture. For the alloy without pre-treatment, annealing at low temperatures resulted in a very strong P texture. As the annealing temperature increased, the strength of the P texture decreased until a weak recrystallization texture was obtained at high temperatures. For the alloy with a pre-treatment of the B condition, the recrystallization texture was mainly characterized by the cube component, and the annealing temperature hardly affected the recrystallization texture. The different behavior of this alloy with and without pre-treatment can be explained by the following considerations.

4.3.1. Formation of recrystallization texture

In considerations of the two fundamental steps for recrystallization, nucleation and growth, recrystallization textures depend on the limited spectrum of preferred nucleus orientations and the growth of nuclei that have the best growth conditions with respect to the surrounding matrix [34]. The recrystallization textures of most Al-alloys are dominated by the cube orientation with some scatter about the RD towards the Goss component. Cube-oriented grains are generally accepted to evolve from band-like structures, the so-called cube-bands, which are already present in the deformed microstructure [35-37]. Another type of recrystallization texture found in aluminum alloys is the R texture, which exhibits almost the same position in Euler space as the former β fiber rolling texture [34,38-40]. It was found that annealing at low temperatures resulted in a strong R texture in cold rolled AA 5182 aluminum alloy [38]. The R oriented grains are formed by nucleation within S oriented grains at the grain boundaries between the deformation bands [34,39,40].

In the case of large particles present in aluminum alloys prior to cold rolling, particle stimulated nucleation (PSN) can be active as another mechanism of recrystallization nucleation [41]. Here, nucleation takes place by rapid subgrain growth within the deformation zones around the large particles. Because of the strong lattice rotations in the vicinity of the particles, generally rather randomly oriented nuclei are observed. PSN is thought to cause a randomizing effect on the total recrystallization texture, and therefore weaken the recrystallization texture [42].

The recrystallization texture of CC AA 3105 aluminum alloy with pre-treatment is characterized by a weak cube component, which is consistent with the observation in most AA 3xxx series aluminum alloys. It is not difficult to understand the formation of recrystallization texture in the alloy with pre-treatment since the alloy exhibits a similar recrystallization behavior to commercial purity aluminum [32]. In this case, the recrystallization texture depends mainly on

the competition of nucleation at cube-bands with particle stimulated nucleation and nucleation at grain boundaries. The relatively weak cube texture with rather high volume fraction of the remainder component can be attributed to the effect of large particles formed during the preheat treatment.

4.3.2. Effect of Zener-particle pinning on recrystallization texture

An important aspect of twin-belt continuous cast processing of aluminum alloys is that CC hot bands have a large amount of elements in solid solution. During annealing at low temperatures after cold rolling, a large amount of dispersoids precipitate at high angle boundaries before the onset of recrystallization and during recrystallization. The concurrent precipitation strongly influences the progress of recrystallization as well as the resulting texture of CC AA 3105 aluminum alloy. The significant difference in the recrystallization kinetics, recrystallized grain structure and recrystallization texture between the alloy with and without pre-treatment naturally points to a Zener-particle pinning effect during recrystallization texture formation.

The texture change during recrystallization is traditionally interpreted in terms of the two rivaling theories of oriented nucleation and oriented growth. In most cases, however, a discussion solely based on one of these two theories fails. Instead, a combination of both theories, i.e. a preferred formation of some orientations at characteristic nucleation sites and a subsequent growth selection of distinct orientations out of this spectrum of nucleus orientations, predominates in recrystallization texture [15,43]. As an alternative to the standard explanation of an oriented growth of grains with a preferred orientation relationship, recently the concept of "orientation pinning" has been proposed, which is based on the fact that the growth of grains which are distinguished by a low probability of being pinned by immobile low-angle or twin grain boundaries is preferred [44]. More recently, Engler [45] has addressed in detail the new approach of orientation pinning.

Form the present observations, it can be concluded that the formation of the P texture is related to concurrent precipitation. In the case of the alloy with pre-treatment, no P texture is created due to the lack of concurrent precipitation. In the case of the alloy without pre-treatment, annealing at low temperatures results in a strong P texture since a large amount of concurrent precipitation occurs. As the annealing temperature increases, the amount of concurrent precipitation decreases. Therefore, the strength of the P texture decreases with increasing annealing temperature.

Daaland and Nes [1] have investigated the evolution of recrystallization texture in commercial Al-Mn-Mg alloys. A similar transition from strong ND rotated cube and P textures to a weak recrystallization texture with increasing the temperature was observed in a deformed supersaturated Al-1.0Mn-0.5Mg alloy. The transition implies that the nucleation and growth of one type of sites are less affected by concurrent precipitation than the other type [1]. At low temperatures, the evolution of recrystallization texture is totally dominated by nucleation and growth of the P oriented grains. As the temperature increases, a shift from a strong P texture to a weak recrystallization texture occurs. The P oriented grains grow slowly, while grains with random orientation grow faster and dominate the recrystallization texture. In more recent work on the recrystallization behavior of supersaturated Al-1.3 wt% Mn alloy, Somerday and Humphreys [5] found that precipitation occurred preferentially at high angle boundaries. It is expected that precipitation concurrent with recrystallization pins preferentially certain boundaries. Therefore, the formation of the P texture should be the result of microgrowth selection caused by Zener-particle pinning. This Zener-particle pinning effect contrasts with the randomizing effect of PSN.

5. Conclusions

The evolution of recrystallization and recrystallization texture during annealing after cold rolling of CC AA 3105 aluminum alloy with different pre-treatments was investigated in detail. The following conclusions are drawn from this study.

(1) The pre-treatment prior to cold rolling strongly affects the recrystallization behavior of CC AA 3105 aluminum alloys. Under the A condition where the hot band was directly cold rolled to 75% reduction, the recrystallization progress is markedly retarded compared with the recrystallization under the B condition, i.e. the pre-treatment at 599°C prior to cold rolling significantly stimulates the recrystallization of CC AA 3105 aluminum alloy. By comparing the TTT diagrams for recrystallization between the A and F conditions, it is concluded that the heat treatment of precipitation at 371°C also significantly stimulates recrystallization. In addition, the preheating temperature also affects the recrystallization behavior of CC AA 3105 aluminum alloy. The recrystallization progress under the D condition is slower than that under the B condition. By comparing the TTT diagrams for recrystallization between the B and G conditions, it is found that the additional heat treatment at 371°C further stimulates the recrystallization of CC AA 3105 aluminum alloy.

(2) Under the A condition, the deformed structure is almost fully recrystallized after annealing at 371°C for 40 days. The microstructure shows coarse elongated recrystallized grains. As the annealing temperature increases, the size of recrystallized grains decreases. At high temperatures, very fine elongated grains were obtained. Under the B condition, fine equiaxed recrystallized grains are observed at all annealing temperatures. The annealing temperature hardly affects the size of recrystallized grains. Under the D and F conditions, the deformed structure is not fully recrystallized at 343°C, 371°C and 399°C although the hardness has decreased to a low value in the curve of hardness and time. Under the G condition, at 316°C, relatively coarse recrystallized grains are observed. As the annealing temperature increases, the size of recrystallized grains decreases. At high temperatures, a fine equiaxed grain structure is obtained. In comparison to the B condition, the recrystallized grains under the G condition are larger than those under the B condition at a given annealing temperature.

(3) The preheat treatment prior to cold rolling strongly affects the evolution of recrystallization texture of CC AA 3105 aluminum alloy. Under the A condition, annealing at low temperatures results in a strong P texture. As the annealing temperature increases, the strength of the P texture decreases. Under the B condition, the recrystallization texture is characterized by a weak cube component, and the annealing temperature does not affect the cube recrystallization texture. Under the D condition, after annealing at 343°C for 2 days, the resulting texture is characterized by a major R component and a minor cube component. The strength of the R texture decreased with increasing annealing temperature. At high temperatures, the recrystallization texture consists of a weak cube component. Under the F condition, after annealing at 343°C for 5 h, the resulting texture is characterized by strong R and P components. The strength of the R and P textures decreases with increasing annealing temperature. At high temperatures, the recrystallization texture consists of a very weak P component. Under the G condition, a stronger cube recrystallization texture is formed than under the B condition.

(4) The transformation kinetics of recrystallization texture during isothermal annealing can be quantified by using the JMAK equation. The n value depends strongly on the pre-treatment prior to cold rolling. Under the A condition, the n value is about 0.35. The low n value can be attributed to the effect of Zener-particle pinning caused by concurrent precipitation. Under the B condition,

the n value of around 2.0 is consistent with other results on aluminum alloys. Under the D and F conditions, the n value varies in the range of 0.4 to 1.4 and 0.8 to 2.8, respectively, and it increases with increasing annealing temperature. Under the G condition, the n value is about 2.3.

(5) Under the A, B and D conditions, the activation energy for recrystallization of CC AA 3105 aluminum alloy is estimated from texture data to be 508, 213 and 188 kJ/mol, respectively. Concurrent precipitation significantly increases the activation energy for recrystallization of CC AA 3105 aluminum alloy. Under the D and F conditions, the apparent activation energy for recrystallization increases with decreasing annealing temperature.

(6) The transition of microstructure and texture observed in CC AA 3105 aluminum alloy without pre-treatment can be explained based on the effect of Zener-particle pinning caused by concurrent precipitation. During annealing at low temperatures, precipitation occurs preferentially at high angle grain boundaries before the onset of recrystallization and during recrystallization. Due to the Zener pinning effect, the coarse elongated grains and the strong P texture are observed. As the annealing temperature increases, recrystallization occurs more rapidly than precipitation, creating less interaction of the two processes. The size of recrystallized grains is reduced, and the strength of the P texture is decreased. At high annealing temperatures recrystallization is finished before substantial precipitation can occur, and a fine grain structure is obtained. In the case of the alloy with pre-treatment, the potential for concurrent precipitation is considerably reduced. In this case, the evolution of recrystallization and recrystallization texture is not affected by concurrent precipitation, but predominately by precipitates present in the as-deformed state.

Part IV. Mechanical Properties of Continuous Cast AA 3105 Aluminum Alloy

Wenchang Liu, James G. Morris, and Chi-Sing Man

1. Introduction

The formability of aluminum sheets depends on the microstructure and texture formed during thermomechanical processing. In the above Parts I to III, the evolution of microstructure and texture during thermomechanical processing has been investigated. In this work, the mechanical properties of CC AA 3105 aluminum alloy were investigated.

2. Experimental

The material used in the present investigation was CC AA 3105 aluminum alloy. The hot band of CC AA 3105 aluminum alloy was preheat treated at (a) 599°C for 6 h, (b) 482°C for 6 h, (c) 371°C for 6 h, and (d) 599°C for 6 h + 371°C for 6 h, and then followed by water quenching. The hot band and preheated hot band were subsequently cold rolled to 75% reduction in thickness, and then annealed at different temperatures for various lengths of time in a salt bath, followed by water quenching.

The tensile properties of CC AA 3105 aluminum alloy sheets were measured. Tensile specimens of 25 mm in length and 6.5 mm in width were machined from the cold rolled and annealed sheets along the RD. The thickness of the tensile samples was equal to that of the cold rolled and annealed sheets. Tensile tests were performed on an Instron testing machine. Yield strength was determined at 0.2% offset strain. Olsen and earing tests were performed to evaluate the formability of these aluminum sheets. The earing of the cold rolled and annealed samples was determined on 36 mm diameter cups. The earing level was calculated using the following equation:

$$\text{Earing level} = \frac{h_{\max} - h_{\min}}{h_{\min}} \tag{7}$$

where $h_{\min}$ is the average height at the valley, and $h_{\max}$ is the average height of the earing peaks.

3. Results and Discussion

3.1. Tensile properties

Table 16 shows the tensile properties (yield strength, YS; ultimate tensile strength, UTS and elongation, EL) of cold rolled CC AA 3105 aluminum alloy with different pre-treatments after annealing at 371°C for different times. The annealing times were selected based on the curves of

Table 16. Tensile properties of cold rolled CC AA 3105 aluminum alloy with different pre-treatments after annealing at 371°C for different times.

Code	Time	X_v (%)	UTS (ksi)	Average UTS (ksi)	YS (ksi)	Average YS (ksi)	EL (%)	Average EL (%)
			30.68		26.97		7.81	
	1 min	0	30.57	30.65	27.03	27.03	7.42	7.55
			30.70		27.10		7.42	
			24.27		16.21		13.28	
A	3 days	50	24.32	24.25	16.15	16.28	13.28	13.15
			24.15		16.48		12.89	
	20 days	75	20.85		10.69		19.14	
			20.77	20.79	10.51	10.55	18.55	18.68
			20.74		10.46		18.36	
			29.07		24.75		8.59	
	5 s	0	29.49	29.48	25.53	25.37	7.03	7.62
			29.88		25.82		7.22	
			24.93		18.40		9.96	
B	50 s	50	24.89	24.92	18.40	18.25	10.16	10.68
			24.94		17.95		11.91	
			20.27		9.14		24.22	
	5 min	100	20.33	20.33	9.46	9.35	21.88	22.92
			20.37		9.45		22.66	
			29.47		24.91		8.40	
	10 s	0	29.58	29.37	25.01	24.71	8.59	8.66
			29.04		24.22		8.98	
			25.71		19.06		10.55	
D	100 s	35	25.41	25.48	18.96	19.00	10.94	11.07
			25.34		18.99		11.72	
			23.46		15.27		14.06	
	2 h	70	23.49	23.49	15.27	15.28	16.80	14.84
			23.50		12.30		13.67	
			30.17		26.09		7.03	
	2 s	0	30.28	30.16	25.82	25.85	7.22	7.23
			30.03		25.62		7.42	
			23.70		13.66		13.48	
F	30 s	40	23.64	23.65	13.71	13.64	13.28	13.34
			23.62		13.55		13.28	
	15 min	80	22.22		12.18		17.38	
			22.12	22.15	12.13	12.07	19.14	18.29
			22.12		11.92		18.35	
			27.09		24.22		6.45	
	2 s	0	27.35	27.20	24.55	24.31	6.05	6.25
			27.15		24.16		6.25	
			20.69		12.06		18.16	
G	20 s	50	21.02	21.20	12.50	12.49	17.19	17.12
			21.89		12.91		16.02	
			19.31		9.15		22.66	
	2 min	100	19.45	19.39	8.97	9.10	23.05	22.66
			19.42		9.17		22.27	

hardness and annealing time, corresponding to the beginning of recrystallization, about 50% recrystallization and complete recrystallization, respectively. However, the deformed structure was not fully recrystallized under the D and F conditions when the hardness decreased to a low level value. Therefore, the volume fraction of recrystallized grains was estimated based on the combination of the measurements of hardness and texture and the observation of microstructure, as shown in Table 16. As recrystallization proceeded, the YS and UTS decreased, whereas the EL increased.

Tables 17-21 show the tensile properties of cold rolled CC AA 3105 aluminum alloy with different pre-treatments after annealing at different temperatures for a selected time. The volume fraction of recrystallized grains is listed in these tables. It is noted that most of the samples were fully recrystallized under these given annealing conditions. Fig. 38 shows the relationship between the tensile properties and annealing temperature for CC AA 3105 aluminum alloy with different pre-treatments. It is seen that the annealing temperature affected the tensile properties of cold rolled CC AA 3105 aluminum alloy sheets after complete recrystallization. Under the A and B conditions, as the annealing temperature increased, the YS, UTS and EL increased. Under the D and F conditions, as the annealing temperature decreased, the YS and UTS increased, whereas the EL decreased. These variations in tensile properties with annealing temperature were caused by partial recrystallization taking place at low temperatures. Under the G condition, as the annealing temperature increased, the YS and UTS hardly changed, while the EL increased. Fig. 39 shows the comparison of the tensile properties of CC AA 3105 aluminum alloy with different pre-treatments. After annealing at 371°C, the alloy with a pre-treatment under the D condition possessed the highest UTS and YS and the lowest elongation. The UTS and YS decreased and the EL increased in the sequence of D→F→A→B→G. After complete recrystallization at 482°C, the alloy without pre-treatment (A condition) possessed the highest UTS and YS and relatively high EL. The UTS and YS decreased in the sequence of A→B→D→ F→G.

Table 17. Tensile properties of cold rolled CC AA 3105 aluminum alloy without pre-treatment (A condition) after annealing at different temperatures for a selected time.

Time	X_v (%)	UTS (ksi)	Average UTS (ksi)	YS (ksi)	Average YS (ksi)	EL (%)	Average EL (%)
371°C 20 days	75	20.85	20.79	10.69	10.55	19.14	18.68
		20.77		10.51		18.55	
		20.74		10.46		18.36	
399°C 8 days	100	20.58	20.55	9.99	10.23	19.14	19.01
		20.52		10.46		19.53	
		20.56		10.23		18.36	
427°C 18 h	100	22.42	22.44	11.11	11.04	20.11	19.53
		22.51		10.92		19.34	
		22.40		11.08		19.14	
454°C 1 min	100	24.52	24.41	13.01	13.02	21.29	21.16
		24.26		13.04		19.92	
		24.46		13.01		22.27	
482°C 10 s	100	25.76	25.89	12.93	13.05	21.48	22.66
		26.01		12.99		22.66	
		25.91		13.24		23.83	

Table 18. Tensile properties of cold rolled CC AA 3105 aluminum alloy with a pre-treatment (B condition) after complete recrystallization at different annealing temperatures.

Time	X_v (%)	UTS (ksi)	Average UTS (ksi)	YS (ksi)	Average YS (ksi)	EL (%)	Average EL (%)
316°C 5 h	100	19.46	19.39	8.83	9.04	21.29	21.68
		19.34		9.15		21.48	
		19.38		9.14		22.26	
371°C 5 min	100	20.27	20.33	9.14	9.35	24.22	22.92
		20.33		9.46		21.88	
		20.37		9.45		22.66	
427°C 1 min	100	22.55	22.24	10.30	10.41	24.41	23.24
		22.24		10.46		22.85	
		21.93		10.48		22.46	
482°C 10 s	100	24.20	23.47	11.07	10.77	24.61	23.44
		23.44		10.62		23.05	
		22.75		10.62		22.66	

Table 19. Tensile properties of cold rolled CC AA 3105 aluminum alloy with a pre-treatment (D condition) after annealing at different temperatures for a selected time.

Time	X_v (%)	UTS (ksi)	Average UTS (ksi)	YS (ksi)	Average YS (ksi)	EL (%)	Average EL (%)
343°C 2 days	40	23.40	23.38	16.02	16.04	13.28	12.76
		23.36		16.02		12.89	
		23.38		16.08		12.11	
371°C 2 h	70	23.46	23.49	15.27	15.28	14.06	14.84
		23.49		15.27		16.80	
		23.50		12.30		13.67	
399°C 1 min	85	23.77	23.73	14.19	13.88	14.84	15.89
		23.74		13.73		16.02	
		23.67		13.73		16.80	
427°C 1 min	100	22.39	22.36	10.95	11.08	20.70	20.31
		22.39		11.18		20.70	
		22.31		11.14		19.53	
454°C 20 s	100	22.44	22.36	10.82	10.80	21.29	21.09
		22.16		10.69		20.90	
		22.47		10.89		21.09	
482°C 10 s	100	22.32	22.24	10.23	10.31	21.68	21.35
		22.32		10.40		20.90	
		22.10		10.30		21.48	

Table 20. Tensile properties of cold rolled CC AA 3105 aluminum alloy with a pre-treatment (F condition) after annealing at different temperatures for a selected time.

Time	X_v (%)	UTS (ksi)	Average UTS (ksi)	YS (ksi)	Average YS (ksi)	EL (%)	Average EL (%)
343°C 5 h	60	22.99	22.84	13.68	13.59	14.65	15.23
		22.82		13.48		16.99	
		22.71		13.62		14.06	
371°C 15 min	80	22.22	22.15	12.18	12.07	17.38	18.29
		22.12		12.13		19.14	
		22.12		11.92		18.35	
399°C 1 min	95	22.30	22.32	11.60	12.02	20.70	19.66
		22.31		12.22		19.34	
		22.36		12.23		18.95	
427°C 1 min	100	21.63	21.55	10.89	10.87	20.70	20.57
		21.63		10.82		20.70	
		21.38		10.92		20.31	
454°C 20 s	100	21.99	21.73	10.67	10.98	20.51	21.29
		21.57		11.26		21.09	
		21.62		10.00		22.27	
482°C 10 s	100	21.98	21.82	10.46	10.43	23.05	22.72
		21.63		10.43		21.68	
		21.85		10.41		23.44	

Table 21. Tensile properties of cold rolled CC AA 3105 aluminum alloy with a pre-treatment (G condition) after complete recrystallization at different annealing temperatures.

Time	X_v (%)	UTS (ksi)	Average UTS (ksi)	YS (ksi)	Average YS (ksi)	EL (%)	Average EL (%)
316°C 2 h	100	18.74	19.02	9.09	9.25	20.70	20.3
		19.10		9.17		21.09	
		19.23		9.48		19.14	
371°C 2 min	100	19.31	19.39	9.15	9.10	22.66	22.66
		19.45		8.97		23.05	
		19.42		9.17		22.27	
427°C 1 min	100	19.81	19.60	9.04	9.21	25.00	24.74
		19.55		9.22		25.39	
		19.45		9.37		23.82	
482°C 10s	100	20.64	20.44	9.48	9.33	26.95	26.69
		20.42		9.27		27.73	
		20.26		9.23		25.39	

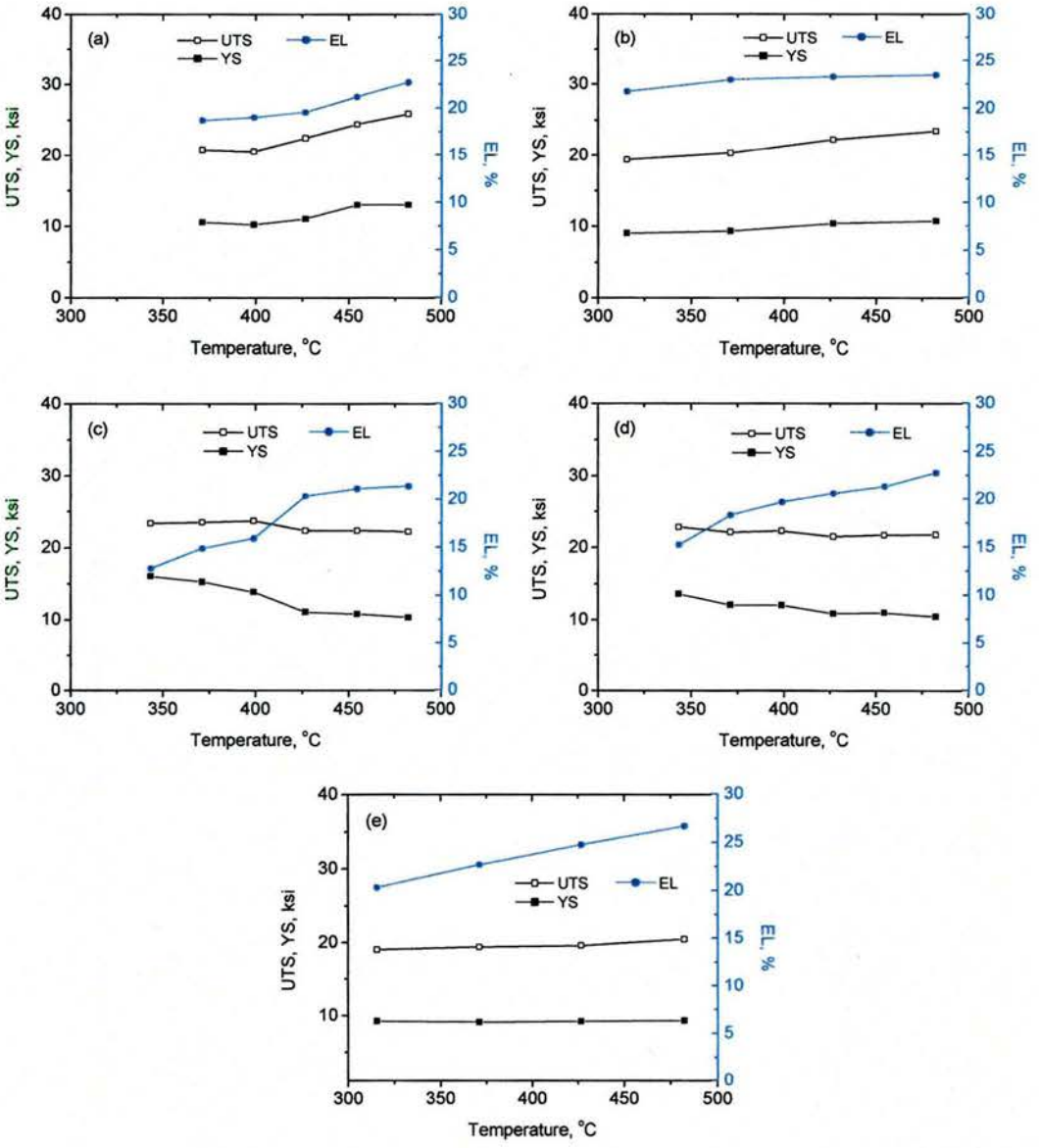

Fig. 38. Relationship between the tensile properties and annealing temperature for CC AA 3105 aluminum alloy. (a) No pre-treatment, (b) 599°C for 6 h, (c) 482°C for 6 h, (d) 371°C for 6 h, and (e) 599°C for 6 h + 371°C for 6 h.

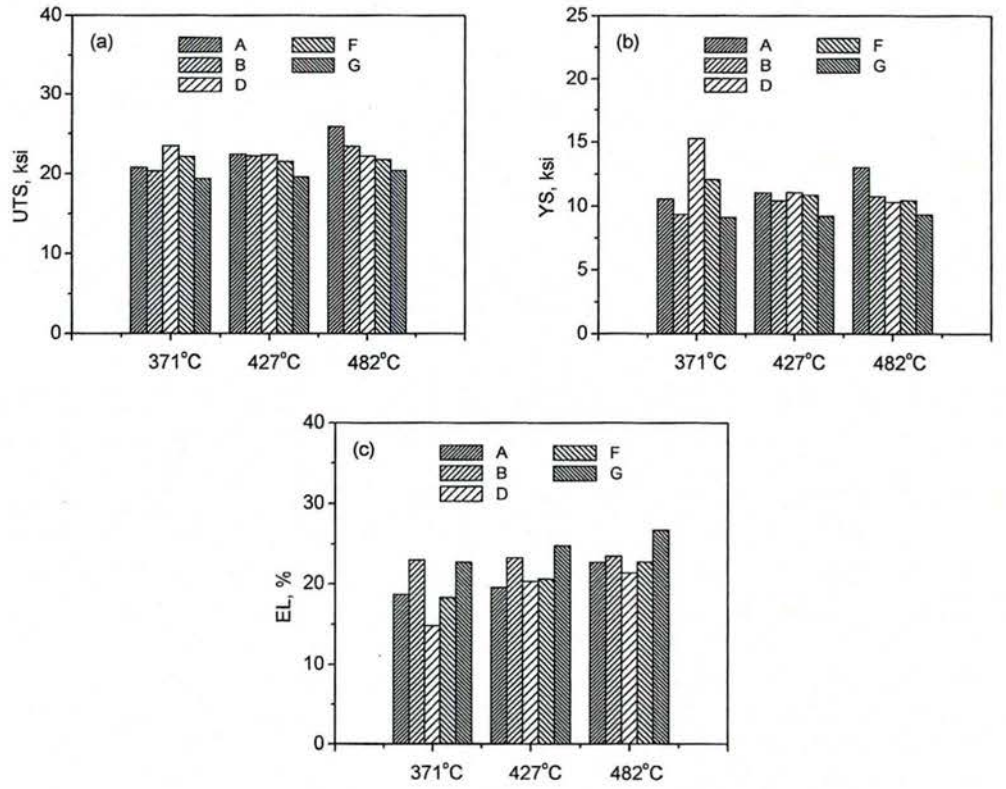

Fig. 39. Comparison of the tensile properties ((a) UTS, (b) YS, (c) EL) of CC AA 3105 aluminum alloy with different pre-treatments.

3.2. Formability

The anisotropy of mechanical properties of aluminum alloy sheets is significantly influenced by the crystallographic texture developed in production. In order to evaluate the effect of pre-treatment on the anisotropy of mechanical properties, the earing values of cold rolled and annealed samples with different pre-treatments were measured. Table 22 shows the earing value of cold rolled CC AA 3105 aluminum alloy with different pre-treatments after annealing at 371°C for different times. It is noted that CC AA 3105 aluminum alloy possessed a significantly high 45° earing value in the recovered state. The pre-treatment prior to cold rolling affected the earing value of these recovered samples. The earing values under the A and F conditions were much higher than those under the B, D and G conditions since the A and F samples possessed a very strong β fiber rolling texture. As recrystallization proceeded, the 45° earing value decreased due to the decrease in the strength of the β fiber rolling texture. Table 23 shows the earing value of cold rolled CC AA 3105 aluminum alloy with different pre-treatments after annealing at different temperatures for a selected time. Fig. 40 shows the relationship between the earing value and annealing temperature for CC AA 3105 aluminum alloy with different pre-treatments. In general, the earing value depended on the annealing temperature. As the annealing temperature decreased,

Table 22. Earing value of cold rolled CC AA 3105 aluminum alloy with different pre-treatments after annealing at 371°C for different times.

Code	Time	Earing, %	Time	Earing, %	Time	Earing, %
A	1 min	12.64	3 day	7.73	20 days	4.66
		12.20		7.67		4.63
B	5 s	6.57	50 s	4.76	5 min	1.64
		6.47		4.08		1.53
D	10 s	6.64	100 s	4.50	2 h	2.94
		6.10		4.38		2.57
F	2 s	11.79	30 s	7.35	15 min	3.87
		11.52		7.01		3.77
G	2 s	6.59	20 s	5.75	2 min	1.13
		6.88		3.97		0.91

Table 23. Earing value of cold rolled CC AA 3105 aluminum alloy with different pre-treatments after annealing at different temperatures for a selected time.

Code	Temp. Time	Earing, %	Temp. Time	Earing, %	Temp. Time	Earing, %	Temp. Time	Earing, %
A					371°C	4.66	399°C	4.27
					20 days	4.63	8 days	5.24
B	316°C	2.18			371°C	1.64		
	5 h				5 min	1.53		
D			343°C	3.16	371°C	2.94	399°C	3.56
			2 days	2.87	2 h	2.57	1 min	2.96
F			343°C	5.49	371°C	3.87	399°C	4.10
			5 h	5.76	15 min	3.77	1 min	4.92
G	316°C	1.11			371°C	1.13		
	2 h				2 min	0.91		

Code	Temp. Time	Earing, %	Temp. Time	Earing, %	Temp. Time	Earing, %
A	427°C	3.74	454°C	4.80	482°C	3.98
	18 h	3.59	1 min	4.61	10 s	3.80
B	427°C	2.17			482°C	2.01
	1 min	1.91			10 s	1.81
D	427°C	2.10	454°C	1.78	482°C	2.13
	1 min	1.98	20 s	1.75	10 s	1.95
F	427°C	4.04	454°C	3.82	482°C	3.85
	1 min	4.02	20 s	3.73	10 s	3.69
G	427°C	1.07			482°C	0.93
	1 min	0.71			10 s	0.90

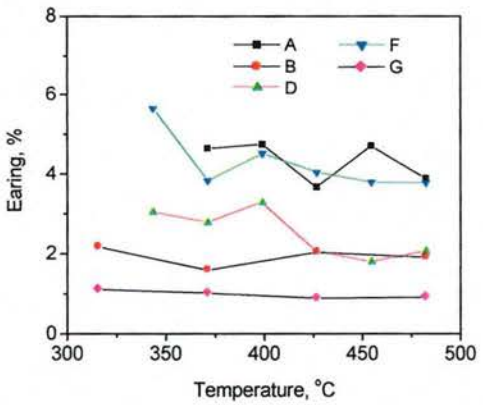

Fig. 40. Relationship between the Earing value and annealing temperature for CC AA 3105 aluminum alloy.

the earing value increased. The pre-treatment prior to cold rolling strongly affected the earing value of CC AA 3105 aluminum alloy. At a given annealing temperature, the A and F samples possessed strong 45° earing values, while the G sample showed the lowest earing value.

The earing value of aluminum alloy sheets depends strongly on the crystallographic texture. It is known that the cube and Goss components produce ears at 0° and 90° to RD, while the β fiber and r-cube component cause 45° earing. The cold rolled sheets possess a strong β fiber rolling texture, leading to high 45° earing values. As recrystallization proceeds, the volume fraction of the β fiber component decreases, which decreases the 45° earing value. After complete recrystallization, the earing profiles depend on recrystallization textures. For the CC AA 3105 aluminum alloy under the A condition, low temperature annealing of cold rolled sheets results in a strong P recrystallization texture and a high 45° earing value. This suggests that the P recrystallization texture produces the 45° ears. As the annealing temperature increases, the strength of the P component decreases markedly, whereas the strengths of the cube, Goss, and R components increase slightly. As a result, the earing value decreases slightly with increasing annealing temperature. For the CC AA 3105 aluminum alloy under the B condition, the recrystallization texture consists mainly of a weak cube recrystallization texture. Since the weak cube component does not balance the effect of the R component, a relatively low 45° earing value is still obtained in this material. In the double pre-treatment case (G condition), the additional heat treatment results in a stronger cube component and further decreases the 45° earing value. For the CC AA 3105 aluminum alloy under the D and F conditions, the high earing value is caused by strong P and R textures.

Table 24 shows the Olsen value of cold rolled CC AA 3105 aluminum alloy with different pre-treatments after annealing at 371°C for different times. The low Olsen value was obtained in the recovered state. The Olsen value increased with increasing the annealing time. Table 25 shows the Olsen value of cold rolled CC AA 3105 aluminum alloy with different pre-treatments after annealing at different temperatures for a selected time. Fig. 41 shows the relationship between the Olsen value and annealing temperature for CC AA 3105 aluminum alloy with different pre-treatments. The G and B samples exhibited higher Olsen value than the A, D and F samples. For the D and F samples, the Olsen value increased with increasing annealing temperature. The Olsen value of aluminum alloy sheets is mainly related to their plasticity. High elongation in the G and B materials results in high Olsen values.

Table 22. Olsen value of cold rolled CC AA 3105 aluminum alloy with different pre-treatments after annealing at 371°C for different times.

Code	Time	Olsen	Time	Olsen	Time	Olsen
A	1 min	0.219	3 day	0.256	20 days	0.278
		0.210		0.246		0.275
B	5 s	0.209	50 s	0.237	5 min	0.315
		0.204		0.237		0.313
D	10 s	0.204	100 s	0.247	2 h	0.268
		0.197		0.246		0.260
F	2 s	0.222	30 s	0.250	15 min	0.288
		0.221		0.244		0.278
G	2 s	0.205	20 s	0.237	2 min	0.312
						0.312

Table 12. Olsen value of cold rolled CC AA 3105 aluminum alloy with different pre-treatments after complete recrystallization at different temperatures.

Code	Temp. Time	Olsen	Temp. Time	Olsen	Temp. Time	Olsen	Temp. Time	Olsen
A					371°C	0.278	399°C	0.289
					20 days	0.275	8 days	0.281
B	316°C	0.324			371°C	0.315		
	5 h	0.316			5 min	0.313		
D			343°C	0.248	371°C	0.268	399°C	0.266
			2 days	0.235	2 h	0.260	1 min	0.261
F			343°C	0.267	371°C	0.288	399°C	0.288
			5 h	0.273	15 min	0.278	1 min	0.286
G	316°C	0.319			371°C	0.312		
	2 h	0.311			2 min	0.312		

Code	Temp. Time	Olsen	Temp. Time	Olsen	Temp. Time	Olsen
A	427°C	0.278	454°C	0.272	482°C	0.274
	18 h	0.275	1 min	0.266	10 s	0.267
B	427°C	0.318			482°C	0.317
	1 min	0.317			10 s	0.307
D	427°C	0.281	454°C	0.296	482°C	0.299
	1 min	0.272	20 s	0.291	10 s	0.296
F	427°C	0.297	454°C	0.297	482°C	0.303
	1 min	0.290	20 s	0.296	10 s	0.297
G	427°C	0.332			482°C	0.333
	1 min	0.330			10 s	0.330

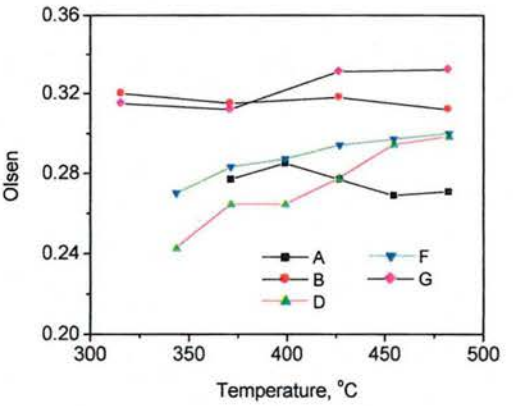

Fig. 41. Relationship between the Olsen value and annealing temperature for CC AA 3105 aluminum alloy.

4. Conclusions

The effect of pre-treatment on the mechanical properties of CC AA 3105 aluminum alloy was investigated. The following conclusions are drawn from this study.

(1) Annealing temperature affects the tensile properties of cold rolled CC AA 3105 aluminum alloy after complete recrystallization. Under the A and B conditions, as the annealing temperature increased, the YS, UTS and EL increased. Under the G condition, as the annealing temperature increased, the YS and UTS hardly changed, while the EL increased.

(2) The heat treatment prior to cold rolling affects the tensile properties of CC AA 3105 aluminum alloy. After annealing at 371°C, the alloy with a pre-treatment under the D condition possesses the highest UTS and YS and the lowest elongation. The UTS and YS decrease and the EL increases in the sequence of D→F→A→B→G. After complete recrystallization at 482°C, the alloy without pre-treatment (A condition) possesses the highest UTS and YS and relatively high EL. The UTS and YS decrease in the sequence of A→B→D→ F→G.

(3) CC AA 3105 aluminum alloy exhibits a significantly high 45° earing value in the recovered state. The pre-treatment prior to cold rolling affects the earing value of these recovered samples. The earing values under the A and F conditions are much higher than those under the B, D and G conditions. As recrystallization proceeds, the 45° earing value decreases due to the decrease in the strength of the β fiber rolling texture. The earing value depends on the annealing temperature. As the annealing temperature decreases, the earing value increases. The pre-treatment prior to cold rolling strongly affects the earing value of CC AA 3105 aluminum alloy. At a given annealing temperature, the A and F samples possess strong 45° earing values, while the G sample exhibits the lowest earing value.

(4) The recovered samples exhibit the lowest Olsen value. The Olsen value increases with increasing the annealing time. After complete recrystallization, the G and B samples exhibit higher Olsen value than the A, D and F samples.

References

[1] O. Daaland and E. Nes: *Acta metall.*, 1996, vol. 44, pp. 1413-35.
[2] H.E. Vatne, O. Engler, and E. Nes: *Mater. Sci. Technol.*, 1997, vol. 13, pp. 93-102.
[3] S. Tangen, K. SjØlstad, E. Nes, T. Furu, and K. Marthinsen: *Mater. Sci. Forum*, 2002, vol. 396-402, pp. 469-74.
[4] K. SjØlstad, O. Engler, S. Tangen, K. Marthinsen, E. Nes: *Mater. Sci. Forum.* 2002, vol. 408-412, pp. 1471-6.
[5] M. Somerday and F.J. Humphreys: *Mater. Sci. Technol.*, 2003, vol. 19, pp. 20-29.
[6] W.C. Liu and J.G. Morris: *Metall. Trans. A*, 2005, vol. 36A, pp. 2829-48.
[7] H.J. Bunge, Texture Analysis in Materials Science, Butterworths, London, 1982.
[8] W.C. Liu and J.G. Morris: *Scripta mater.*, 2002, vol. 47, pp. 743-48.
[9] W.C. Liu and J.G. Morris: *Mat. Sci. Eng.*, 2003, vol. A339, pp. 183-93.
[10] W.C. Liu and J.G. Morris: *Metall. Trans. A*, 2004, vol. 35A, pp. 265-77.
[11] W.C. Liu, D. Juul Jensen, J.G. Morris: *Acta metall.*, 2001, vol. 49, pp.3347-67.
[12] J. Hirsch and K. Lücke: *Acta metall. mater.*, 1988, vol. 36, pp. 2863-82.
[13] O. Engler, J. Hirsch, and K. Lücke: *Acta metall. mater.*, 1989, vol. 37, pp. 2743-53.
[14] P.A. Hollinshead and T. Sheppard: *Metall. Trans. A*, 1989, vol. 20A, pp. 1495-507.
[15] K. Lücke and O. Engler: *Mater. Sci. Technol.*, 1990, vol. 6, pp. 1113-30.
[16] O. Engler, P. Yang, and X.W. Kong: *Acta mater.*, 1996, vol. 44, pp. 3349-69.
[17] W. C. Liu, T. Zhai, and J.G. Morris: *Scripta mater.*, 2004, vol. 51, pp. 83-88.
[18] O. Engler and K. Lücke: *Mater. Sci. Eng. A*, 1991, vol. 148, pp. 15-23.
[19] M. Hölscher, D. Raabe, and K. Lücke: *Acta metall. mater.*, 1994, vol. 42, pp. 879–886.
[20] D. Raabe: Acta metal. Mater., 1995, vol. 43, pp. 1023-8.
[21] D. Raabe, Z. Zhao and W. Mao: *Acta mater.*, 2002, vol. 50, pp. 4379-4394.
[22] J. Hirsch, E. Nes, and K. Lücke: *Acta metall.*, 1987, vol. 35, pp. 427-38.
[23] W.C. Liu, T. Zhai, C.-S. Man, B. Radhakrishnan, and J.G. Morris: *Philosophical Magazine*, 2004, vol. 84, pp. 3305-21.
[24] O. Engler, M. Crumbach, and S. Li: *Acta mater.*, 2005, vol. 53, pp. 2241-2257.
[25] W.C. Liu, C.-S. Man, J. G. Morris: *Scripta mater.*, 2001, vol. 45, pp. 807-14.
[26] D. Raabe, Z. Zhao, and F. Roters: *Scripta mater.*, 2004, vol. 50, pp. 1085-1090.
[27] W.C. Setzer and J.G. Morris: Trans ASM, 1964, vol. 57, pp. 589-602.
[28] J.G. Morris: Trans ASM, 1966, vol. 59, pp. 1006-9.
[29] N. Hansen, T. Teffers, and J.K. Kjems: Acta metall., 1981, vol. 29, pp. 523-33.
[30] W.C. Liu, T. Zhai, C.-S. Man, and J.G. Morris: Scripta mater., 2003, vol. 49, pp. 539-45.
[31] T. Furu, H.R. Shercliff, G.J. Baxter, and C.M. Sellars: Acta mater., 1999, vol. 47, pp. 2377-89.
[32] R.A. Vandermeer and D. Juul Jensen: Acta metall., 2001, vol. 49, pp. 2083-94.
[33] W.C. Liu, Z. Li, T. Zhai, C.-S. Man, and J.G. Morris: In: Jin Z, Beaudoin A, Bieler TR, Radhakrishnan B, (Eds.), Hot Deformation of Aluminum Alloy, TMS, San Diego, California, 2003, p. 125-34.
[34] O. Engler, H.E. Vatne, and E. Nes: Mater. Sci. Eng. A, 1996, vol. 205, pp. 184-94.
[35] A.L. Dons and E. Nes: *Mater. Sci. Technol.*, 1986, vol. 2, pp. 8-18.
[36] J. Hjelen, R. Ørsund, and E. Nes: Acta metall. mater., 1991, vol. 39, pp. 1377-404.
[37] R.D. Doherty, K. Kashyap, and S. Panchanadeeswaran: Acta metall. mater., 1993, vol. 41, pp. 3029-53.
[38] W.C. Liu, T. Zhai, and J.G. Morris: Mater. Sci. Eng. A, 2003, vol. 358, pp. 84-93.
[39] O. Engler: Metall. Trans. A, 1999, vol. 30A, pp. 1517-27.

[40] A. Duckham, O. Engler, and R.D. Knutsen: Acta mater., 2002, vol. 50, pp. 2881-93.
[41] F.J. Humphreys: Acta metall., 1977, vol. 25, pp. 1323-44.
[42] D. Juul Jensen, N. Hansen, and F.J. Humphreys: Acta metall., 1985, vol. 33, pp. 2155-62.
[43] O. Engler, J. Hirsch, and K. Lücke: *Acta metall. Mater.*, 1995, vol. 43, pp. 121-38.
[44] D. Juul Jensen: Acta metall. mater., 1995, vol. 43, pp. 4117-29.
[45] O. Engler: Acta mater., 1998, vol. 46, pp. 1555-68.